Supporting Information

Synthesis, Structure, and Photophysical and Electrochemical Properties of a π-Stacked Polymer

Tamaki Nakano[†,††,*] and Tohru Yade[††]

PRESTO, Japan Science and Technology Corporation (JST) and Graduate School of Materials Science, Nara Institute of Science and Technology (NAIST), Takayama-cho 8916-5, Ikoma, Nara 630-0101, Japan

Experimental Details

Materials. 9-Fluorenylmethanol (Wako chemicals, >98%) and potassium tert-butoxide (Wako, 85%) were used as obtained. Fluorene (Wako, >95%) was recrystallized from hexane (mp 117.9 - 118.3°C). *n*-Butyllithium (*n*-BuLi) (Nacalai, 1.6 M), methyllithium (MeLi) (Kanto chemical, 1.1 M, a diethyl ether solution), and phenyllithium (PhLi) (Kanto, 1.0 M, a cyclohexane-diethyl ether solution) were used as obtained. Iodoethane (Wako, >98%) and benzyl bromide (Wako, >98%) were dried over CaH_2 and distilled immediately before use. Tetrahydrofuran (THF) (Wako) was refluxed over sodium benzophenone ketyl, distilled and stored on $LiAlH_4$ under N_2 atmosphere, and distilled under vacuum immediately before use.

Synthesis of DBF. DBF was synthesized according to the literatures[S1,S2] with modifications. 9-Fluorenylmethanol (10.7 g, 54.5 mmol) dissolved in methanol (70 mL) was mixed with a solution of potassium tert-butoxide (8.67 g, 77.3 mmol) in methanol (40 mL). The solution was stirred at 60°C for 20 min. The organics were extracted with a hexane-water mixture, and the hexane layer was washed with water until the wash water was neutral. Polymeric impurities were removed from the hexane layer by filtration using Celite. Removal of solvent gave colourless crystals: 8.23 g (84.9%). The monomer (purity 98.4% by ^{1}H NMR) was stored as a dry THF solution under N_2 in the dark at -20°C.

Preparation of 9-Fluorenyllithium (9-FlLi). The reaction was carried out in a glass ampule sealed with a glass-made three-way stopcock attached to the ampule via a ground joint. The joint was completely sealed with high-vacuum grease. The ampule was flame-dried under high vacuum and flushed with N_2 immediately before use. Fluorene (838 mg, 5.00 mmol) was placed in the glass ampule, dried under high vacuum for 10 min, and purged with N_2. THF (6.0 mL) was introduced using a syringe to dissolve the fluorene. *n*-BuLi (1.6 M hexane solution, 3.1 mL, 5.0 mmol) was added to the solution at room temperature. The resulting deep-orange 9-FlLi solution (0.50 M) was used as an initiator after standing for 10 min at room temperature.

Synthesis of Oligomers. The glassware setup was the same as that for the 9-FlLi synthesis. A typical procedure is described for run 6 in Table 1. A THF solution of DBF (0.672 M THF solution, 14.9 mL, 10.0 mmol) and dry THF (33.1 mL) were introduced to the ampule with a syringe. The polymerization was initiated by adding the MeLi solution (1.8 mL, 2.0 mmol) to the monomer solution cooled at -78°C. After 48 h of reaction, the monomer conversion ratio was monitored by ^{1}H NMR analysis of an aliquot (ca. 0.1 mL) of the reaction mixture dissolved in $CDCl_3$ (0.6 mL). Monomer conversion was found to be 84% based on the intensity of the olefinic proton signal (s,

6.0 ppm) using the solvent signal (m, 3.7 ppm) as an internal reference. Iodoethane (2.0 ml, 25 mmol) was added to the reaction mixture. The reaction mixture was fractionated into THF-soluble and –insoluble parts with a centrifuge. Removal of the solvent from the THF-soluble parts afforded the DBF oligomers (1.42 g, yield 74.7 %) as a pale yellow solid.

Measurements. The ^{1}H NMR spectra were recorded on a JEOL JNM-ECP600NK or JEOL ECP500 spectrometer (600 and 500 MHz, respectively, for ^{1}H measurement).

Analytical scale SEC was carried out using a chromatographic system consisting of a JASCO PU-980 chromatographic pump, a JASCO UV-975 UV detector (254 nm), and a JASCO RI-930 RI detector equipped with two PL-Oligopore columns (30 x 0.72(i.d.) cm) (Polymer Laboratories) connected in series. Preparative SEC separation of oligomers was performed using a JAI LC-908 preparative recycle chromatograph equipped with JAIGEL-1H and JAIGEL-2H columns connected in series.

MALDI-mass spectra were taken on a Voyager DE-STR spectrometer equipped with a N_2 laser (337 nm, 3 ns pulse duration, frequency up to 20 Hz) under vacuum (sample chamber pressure 5.5 x 10^{-7} Torr) using the reflector mode (acceleration voltage 20,000 V). The excitation laser power was set to 3000. Samples were prepared by mixing a $CHCl_3$ solution of polymer (concentration 10 mg/mL, 1 μL), a $CHCl_3$ solution of dithranol (concentration 10 mg/mL, 20 μL), and a methanol solution of silver trifluoroacetate (concentration 0.1 mg/mL, 1 μL) and drying the mixed solution in a sample well on a gold-plated sample slide under air flow.

Single crystal X-ray data were collected at room temperature on a Rigaku R-AXIS RAPID Imaging Plate diffractometer using Mo-Kα radiation (λ = 0.71073 Å) monochromated by graphite. All calculations were performed using the teXsan software package (version 1.10b).

Absorption and emission spectra were measured at room temperature in a 1-cm quartz cell with a JASCO V-550 spectrophotometer and a JASCO FP-777W fluorescence spectrophotometer, respectively. Samples in the THF solvent were degassed by N_2 bubbling for 10 min.

Cyclic voltammetry experiments were performed with a Hokuto-Denko HSV-100 electrochemical analyzer in a THF solution containing tetrabutylammonium perchlorate as a supporting electrolyte (0.1 M) under N_2 flow. Sample solutions were degassed by N_2 bubbling for 10 min prior to the measurement. All measurements were carried out at room temperature with a conventional three-electrode configuration consisting of a platinum working electrode, an auxiliary platinum electrode, and a Ag/AgCl reference

electrode at a sweep rate of 100 mV/s. The half-wave potential ($E_{p/2}$) values were determined as the potential at the current that was half of diffusion limiting current.

Computer Simulation. **A** Monte Carlo conformational search was carried out using MacroModel 6.0 software (Schrödinger).[S3] The relative arrangements of the fluorene moieties were fixed and the main-chain torsions were changed at an interval of 60° in generating initial geometries. Each conformer generated in the Monte Carlo process was fully minimized using MM3[S4] or MMFF94s[S5] force field until the RMS residue went below 0.05 kcal/mol/Å or 1000 iterations were achieved. Conformers most frequently found with in 15kJ/mol energy range from the global minimum were considered to be the most stable ones.

Molecular mechanics structure optimization was effected using the COMPASS[S6] force field implemented in the Discover module of the Material Studio 2.0 (Accelrys) software package with the Fletcher-Reeves[S7] conjugate gradient algorithm until the RMS residue went below 0.01 kcal/mol/Å. Molecular dynamic simulation was performed under a constant NVT condition in which the numbers of atoms, volume, and thermodynamic temperature were held constant. Berendsen's thermocouple[S8] was used for coupling to a thermal bath. The step time was 1 fs and the decay constant was 0.1 ps. Conformations obtained through MD simulation were saved in trajectory files at every 5 or 10 ps and were optimized by MM simulation.

^{1}H NMR chemical shift simulations by the DFT method[S9] were performed using the DGauss software in the CaChe package (Fujitsu). The models were optimized with MOPAC (Fujitsu) software by the semi empirical PM5[S10] method prior to the NMR calculations. NMR simulation was carried out using B88[S11] exchange and LYP[S12] correlation functionals with a DZVP basis set. LORG approximation was applied for the shift simulation to avoid the gauge problem.

Reference

(S1) Greenhow, E. J.; McNeil, D.; White, E. N. *J. Chem. Soc.* **1952**, 986-992.

(S2) More O'Ferrall, R. A.; Slae, S. *J. Chem. Soc. Chem. Commun.* **1969***,* 486-487.

(S3) Mohamadi, F.; Richards, N. G. J.; Guida, W. C.; Liskamp, R.; Lipton, M.; Caufield, C.; Chang, G.; Hendrickson, T.; Still, W. C. *J. Comput. Chem.* **1990**, *11*, 440-467.

(S4)Allinger, N. L.; Yuh, Y. H.; Lii, J.-H. *J. Am. Chem. Soc.* **1989**, *111*, 8551-8566.

(S5) Halgren, T. A. *J. Comput. Chem.* **1999**, *20*, 730-748.

(S6) Sun, H. *J. Phys. Chem.* **1998**, *102*, 7338-7364.

(S7) Fletcher, R.; Reeves, C. M. *Comput. J.* **1964**, *7*, 149-154.

(S8) Berendsen, H. J. C.; Postma, J. P. M.; van Gunsteren, W. F.; DiNola, A.; Haak, J. R. *J. Chem. Phys.* **1984**, *81*, 3684-3690.
(S9) Koch, W.; Holthausen, M. C. *A Chemist's Guide to Density Functional Theory:* Wiley-VCH; New York, 2000, pp 197-216.
(S10) Stewart, J. J. P. MOPAC2002 software; Fujitsu Limited: Tokyo, Japan, 2001.
(S11) Becke, A. D. *Phys. Rev., A* **1988**, *38*, 3098-3100.
(S12) Lee, C.; Yang, W.; Parr, R. G. *Phys. Rev., B* **1988**, *37*, 785-789.

Table S1. Purity of Oligo(DBF)s Isolated by Preparative SEC[a]

	lower-molecular-weight fraction (%)	main fraction (%)	higher-molecular-weight fraction (%)
1 (n=2)	–	>99	–
1 (n=3)	–	95.2	4.8
1 (n=4)	–	>99	–
1 (n=5)	–	>99	–
1 (n=6)	3.1	95.5	0.4
1 (n=7)	–	98.6	1.4
1 (n=8)	0.5	98.1	1.4
2 (n=2)	–	95.1	4.9
2 (n=3)	1.6	97.8	0.6
2 (n=4)	0.8	98.5	0.8
2 (n=5)	3.7	94.9	1.4
2 (n=6)	2.3	96.3	1.4
2 (n=7)	3.3	94.5	2.3
2 (n=8)	2.8	91.8	5.4

[a]Determined by analytical SEC using two OligoPore columns connected in series (eluent THF).

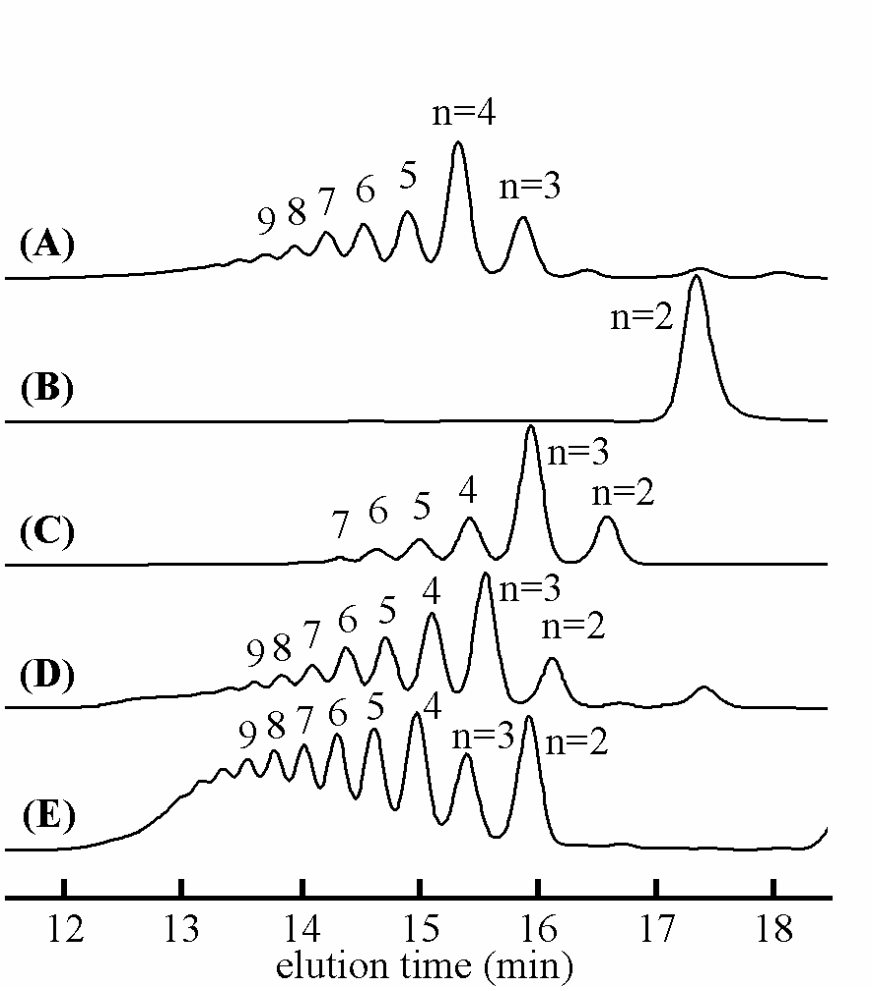

Figure S1. SEC curves of oligo(DBF)s **1** (Table 1, entry 1) (A), **1** (Table 1, entry 2) (B), **2** (Table 1, entry 3) (C), **3** (Table 1, entry 4) (D), **5** (Table 1, entry 6) (E) [column, two PL OligoPore Columns (30 x 0.72 (i.d.) cm) (Polymer Laboratories); eluent, THF; flow rate, 1.0 ml/min].

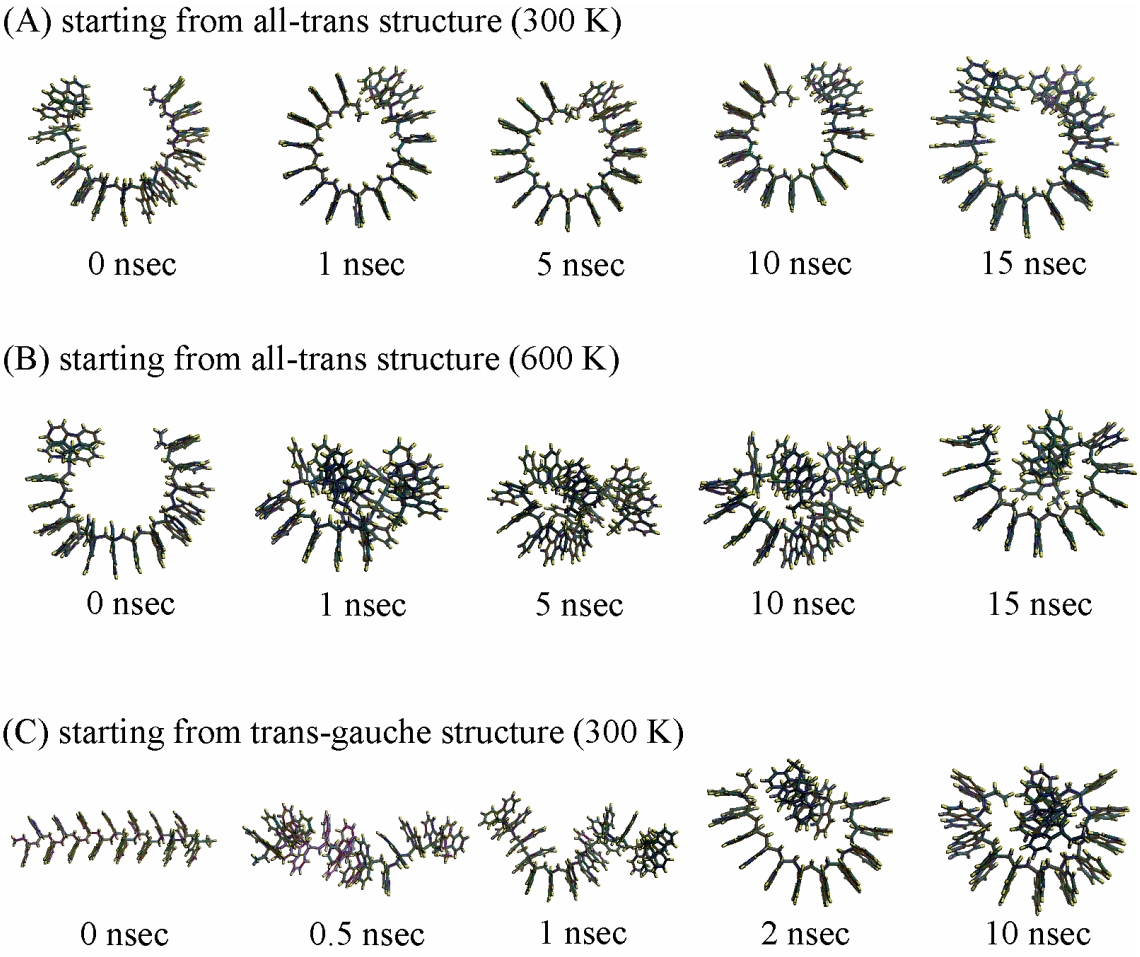

Figure S2. Conformations of **2** of n = 15 observed during the MD simulations: those starting from an all-trans structure at 300 K (A), those starting from an all-trans structure at 600 K (B), and those starting from an alternating trans-gauche structure at 300 K (C).

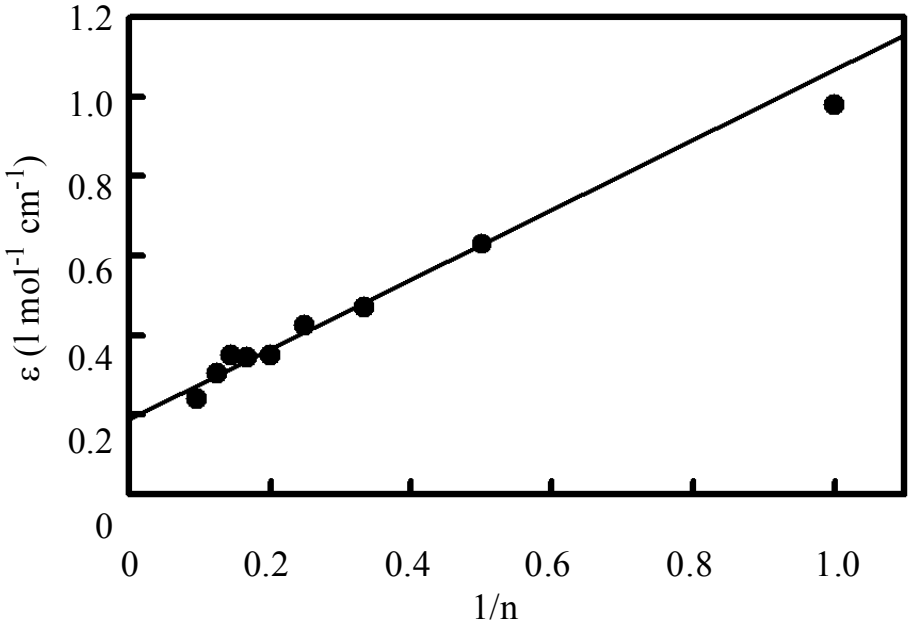

Figure S3. Molar extinction coefficient-vs.-1/n plots for the longest wavelength absorption maxima of oligo(DBF)s **2**. Extrapolation of the plot to 1/n = 0 gave 1890 l mol^{-1} cm^{-1} for a polymer with an infinite number of fluorene moiety. Data at 1/n = 1 are for 9-methylfluorene, and those at 1/n = 0.0962 are for a polymer (*Mn* = 1890 (vs. oligo(DBF)), $\bar{n}$ = 10.4).

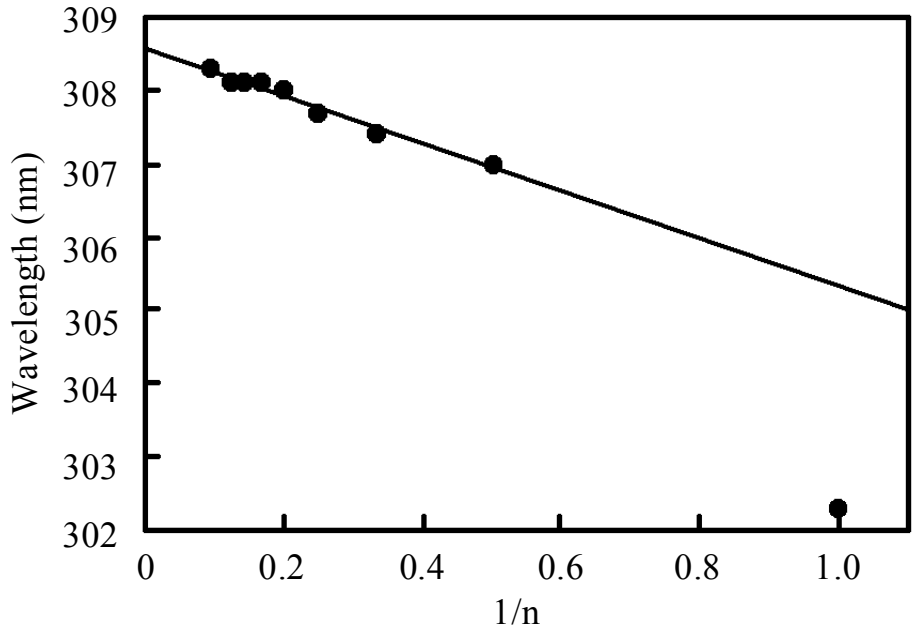

Figure S4. Wavelength-vs.-1/n plots for the longest wavelength absorption maxima of oligo(DBF)s **2**. Extrapolation of the plot to 1/n = 0 gave 308.6 nm for a polymer with an infinite number of fluorene moiety. Data at 1/n = 1 are for 9-methylfluorene, and those at 1/n = 0.0962 are for a polymer (*Mn* = 1890 (vs. oligo(DBF)), $\bar{n}$ = 10.4).

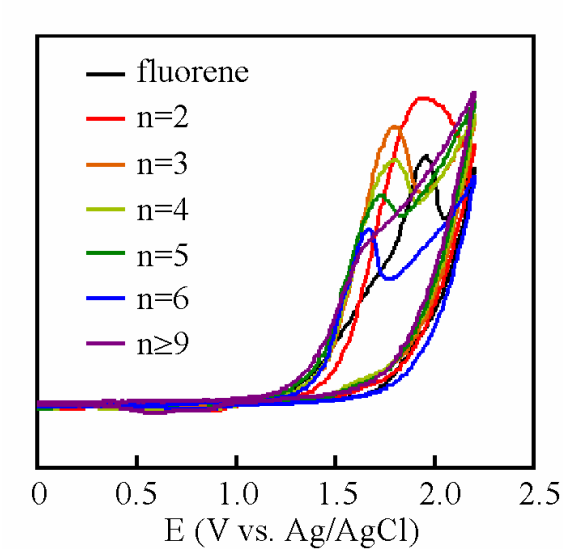

Figure S5. Cyclic voltammograms of oligo(DBF)s (**2**) and fluorene.

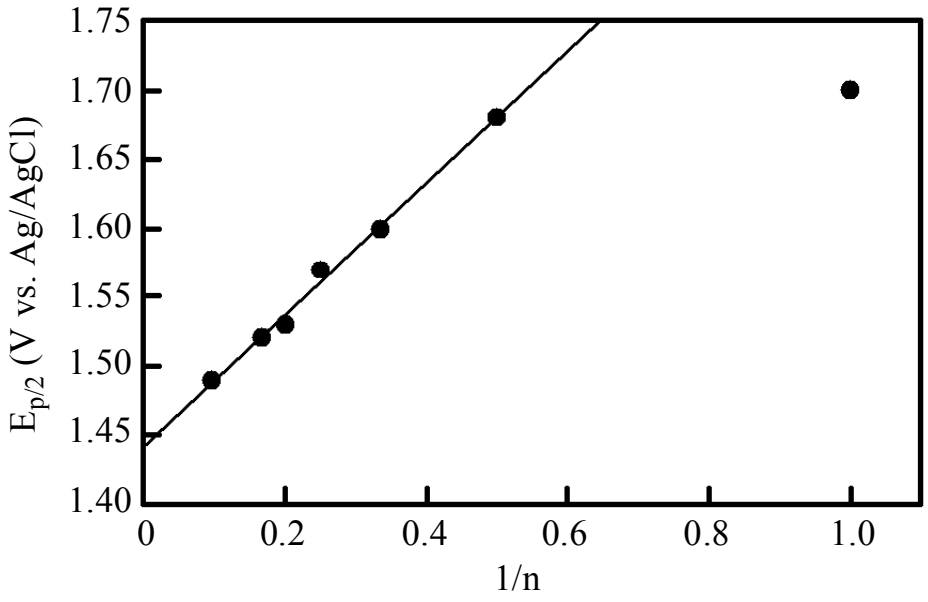

Figure S6. Half wave potential-vs.-1/n plots for the longest wavelength absorption maxima of oligo(DBF)s **2**. Extrapolation of the plot to 1/n = 0 gave 1.44 V vs. Ag/AgCl (1.40 V vs. SCE) for a polymer with an infinite number of fluorene moiety. Data at 1/n = 1 are for fluorene, and those at 1/n = 0.0962 are for a polymer (*Mn* = 1890 (vs. oligo(DBF)), $\bar{n}$ = 10.4).

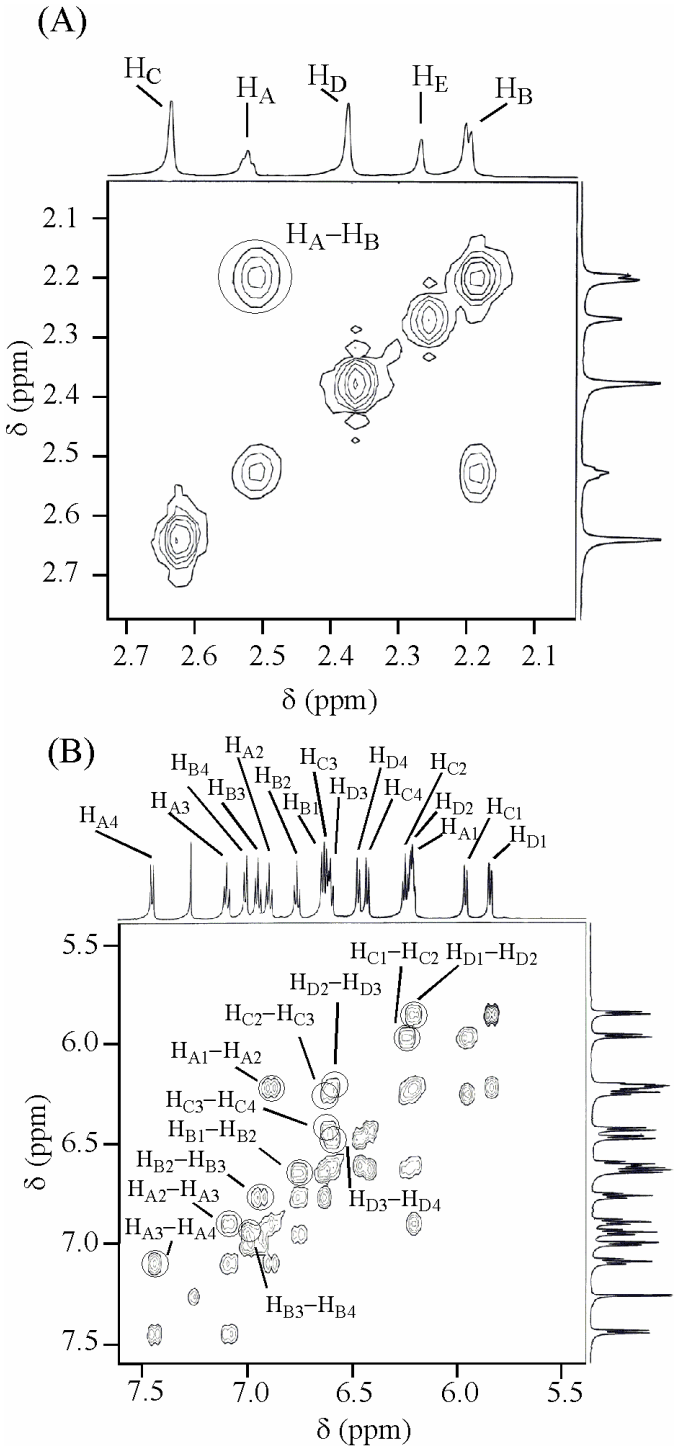

Figure S7. H-H COSY spectra of oligo(DBF) **1** of n = 8: alkyl region (A) and aromatic region (B) (500 MHz, $CDCl_3$, r.t.).

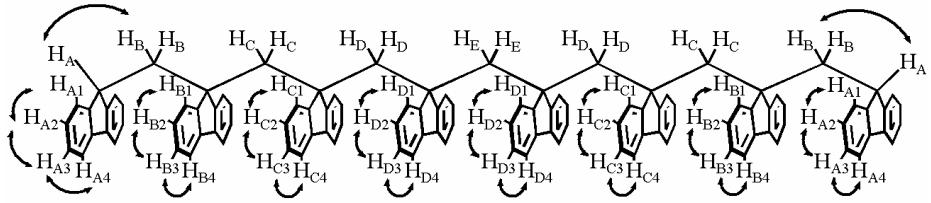

1 of n=8

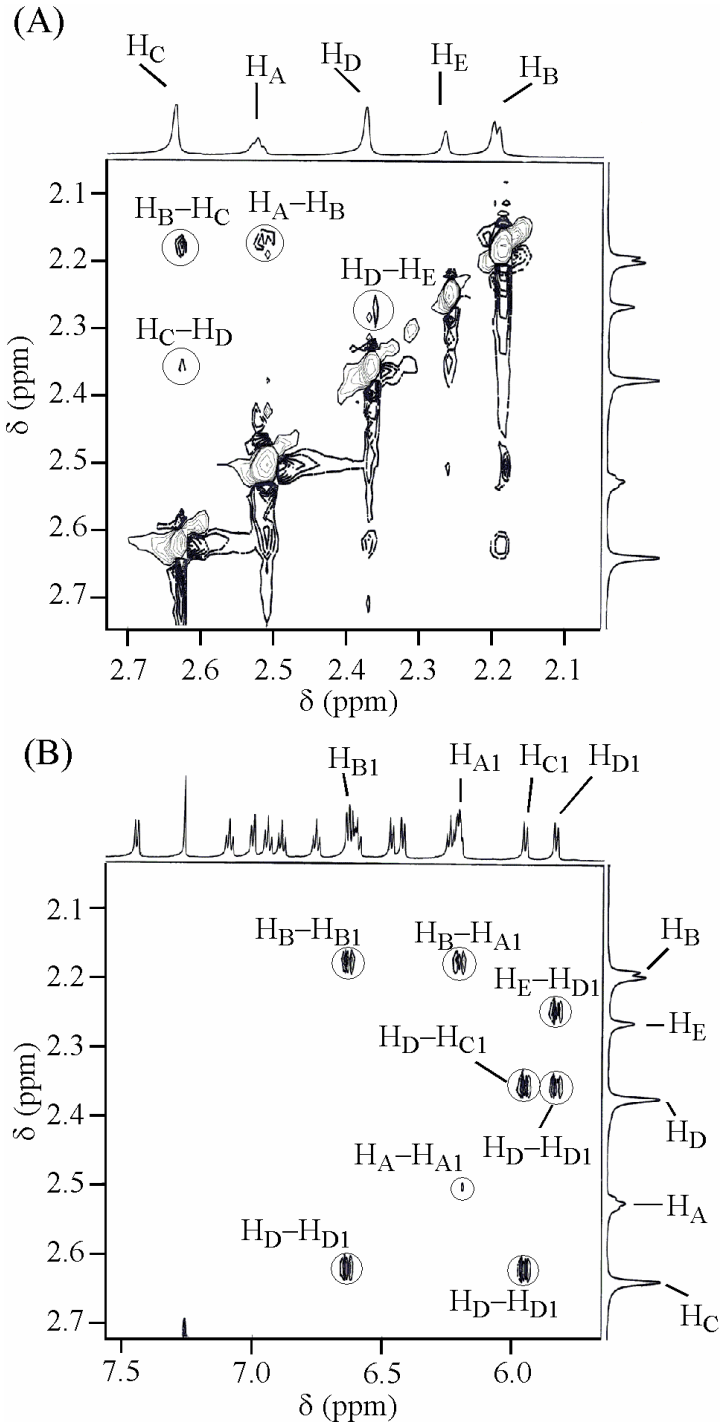

Figure S8. NOESY spectra of oligo(DBF) **1** of n = 8: alkyl-alkyl region (A) and alkyl-aromatic region (B) (500 MHz, $CDCl_3$, r.t.).

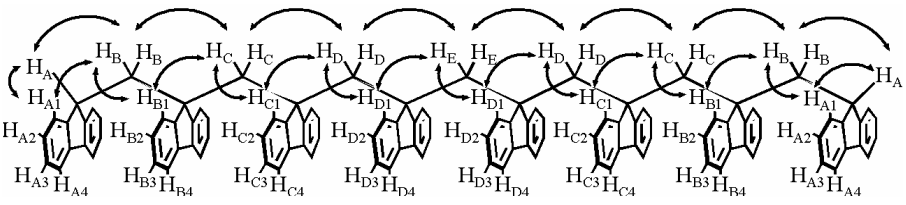

1 of n=8

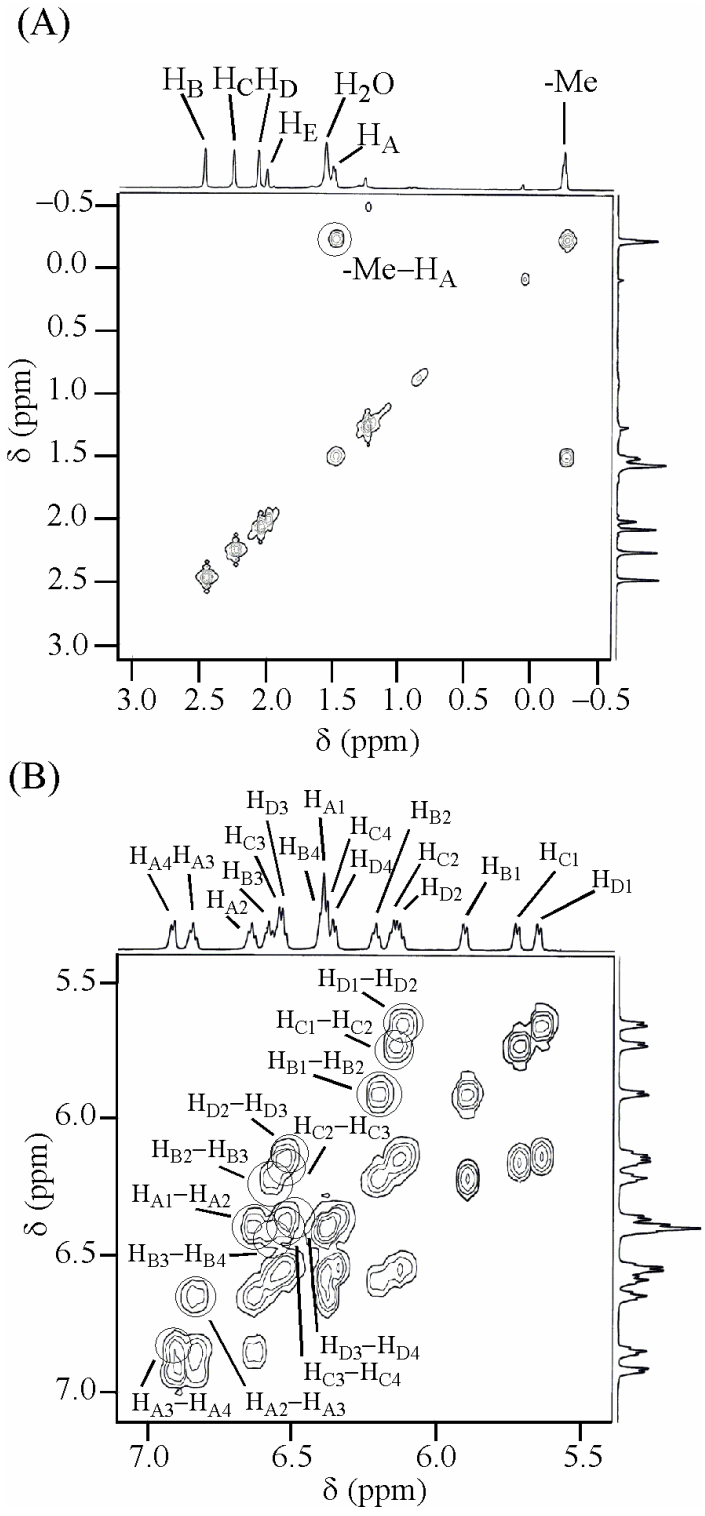

Figure S9. H-H COSY spectra of oligo(DBF) **2** of n = 8: alkyl region (A) and aromatic region (B) (500 MHz, $CDCl_3$, r.t.).

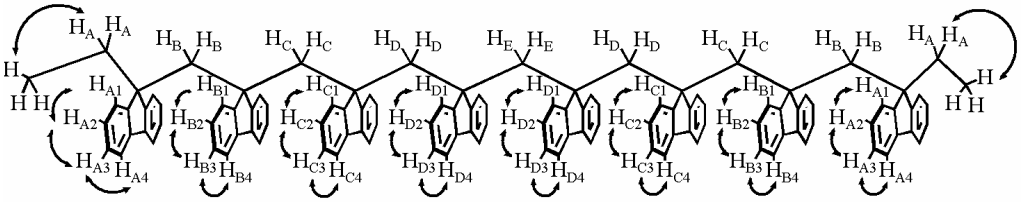

2 of n=8

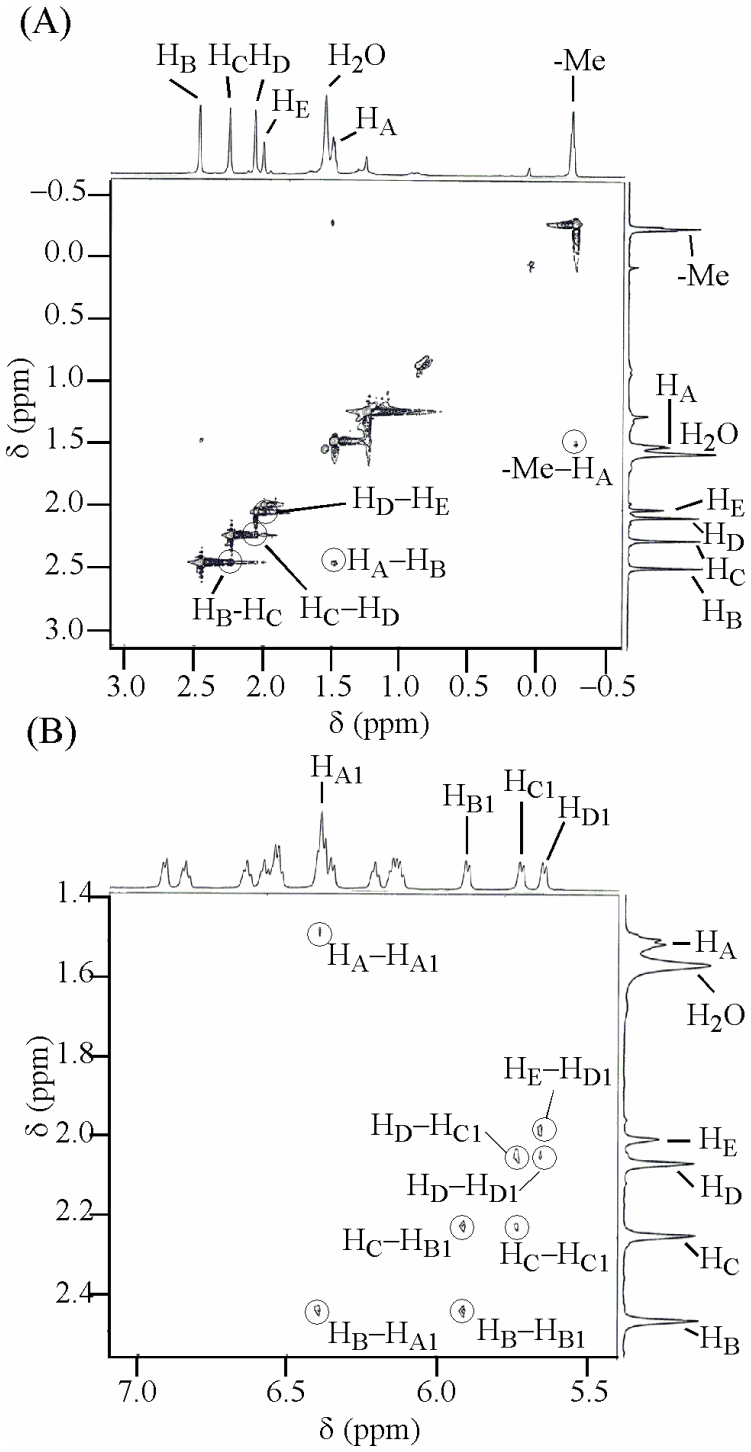

Figure S10. NOESY spectra of oligo(DBF) **2** of n = 8: alkyl-alkyl region (A) and alkyl-aromatic region (B) (500 MHz, $CDCl_3$, r.t.).

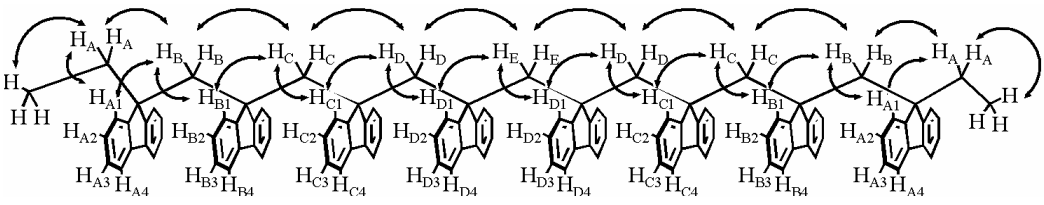

2 of n=8

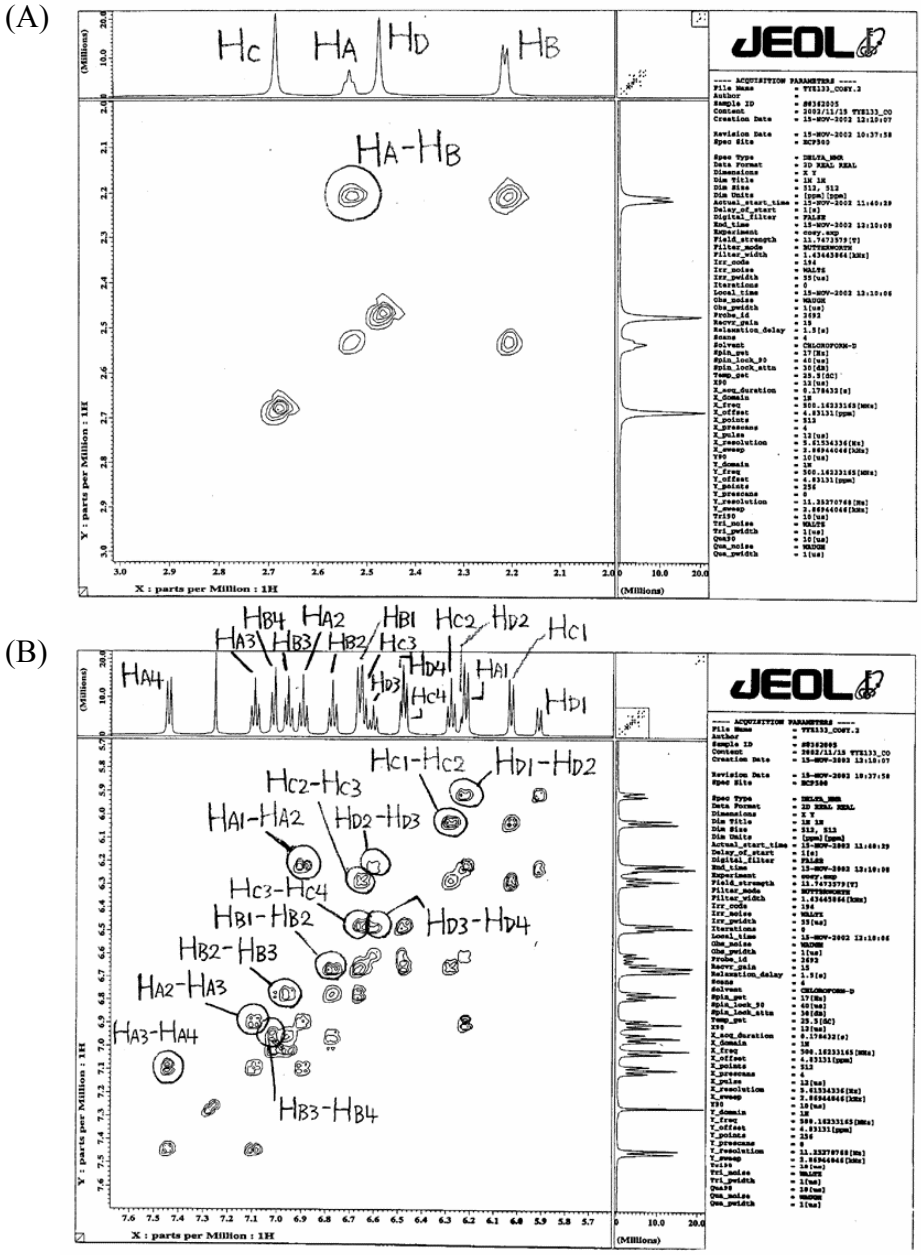

Figure S11. H-H COSY spectra of oligo(DBF) **1** of n = 7: alkyl region (A) and aromatic region (B) (500 MHz, $CDCl_3$, r.t.).

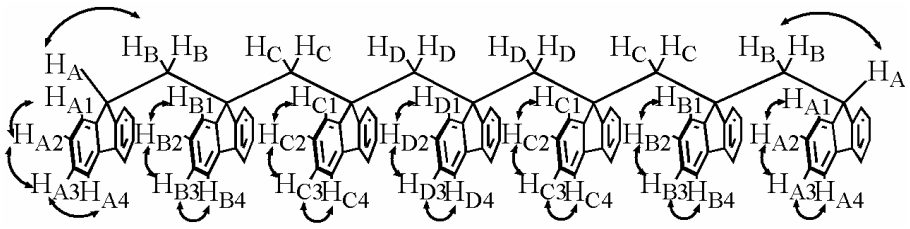

1 of n=7

(A)

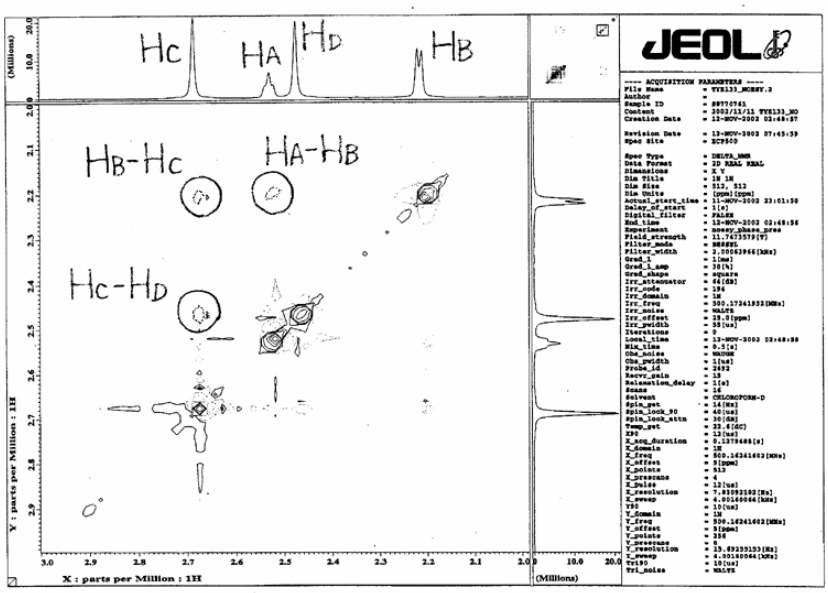

(B)

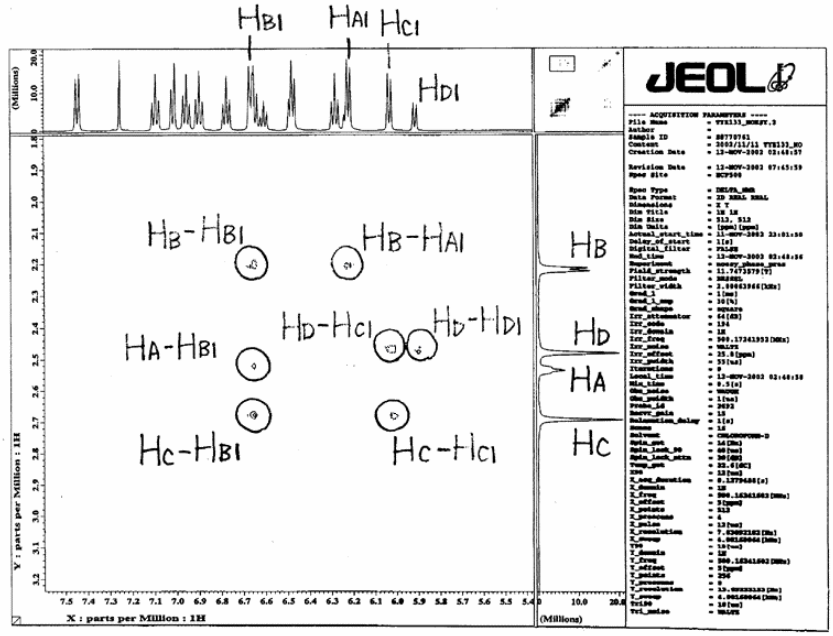

Figure S12. NOESY spectra of oligo(DBF) **1** of n = 7: alkyl-alkyl region (A) and alkyl-aromatic region (B) (500 MHz, $CDCl_3$, r.t.).

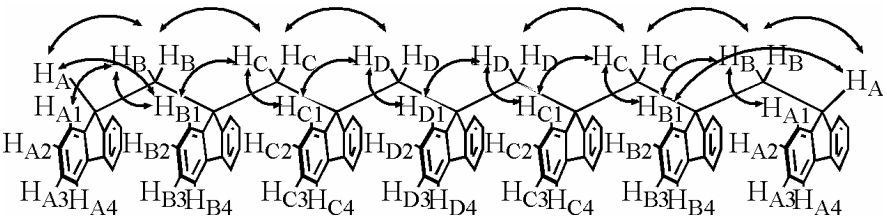

1 of n=7

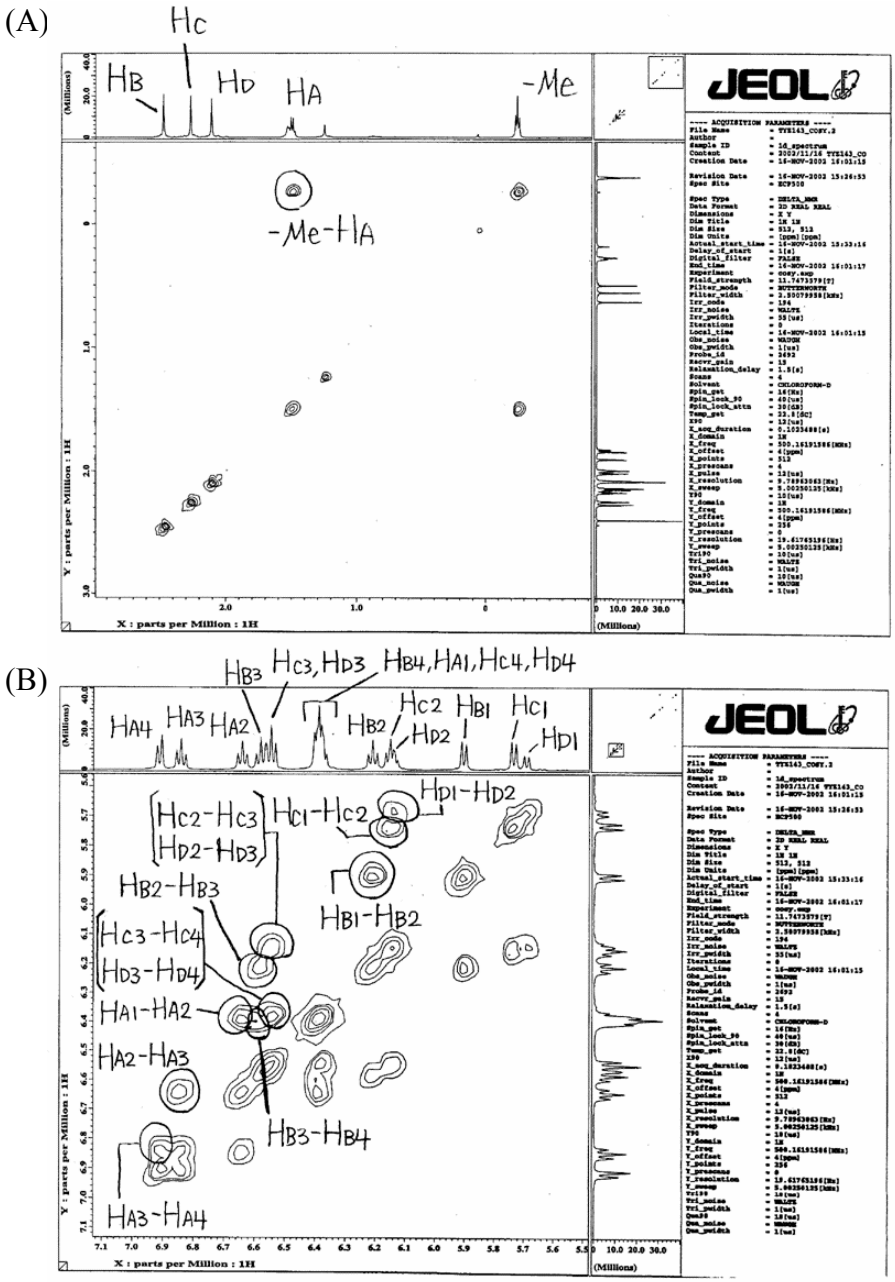

Figure S13. H-H COSY spectra of oligo(DBF) **2** of n = 7: alkyl region (A) and aromatic region (B) (500 MHz, $CDCl_3$, r.t.).

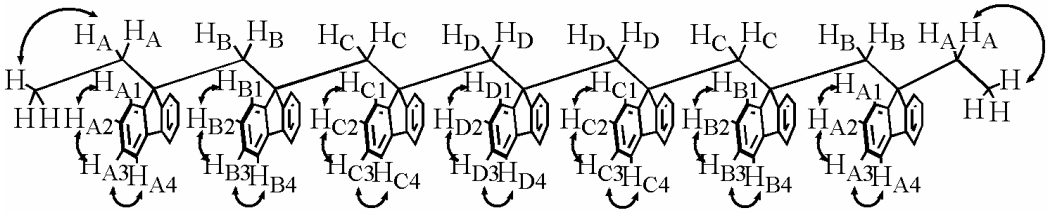

2 of n=7

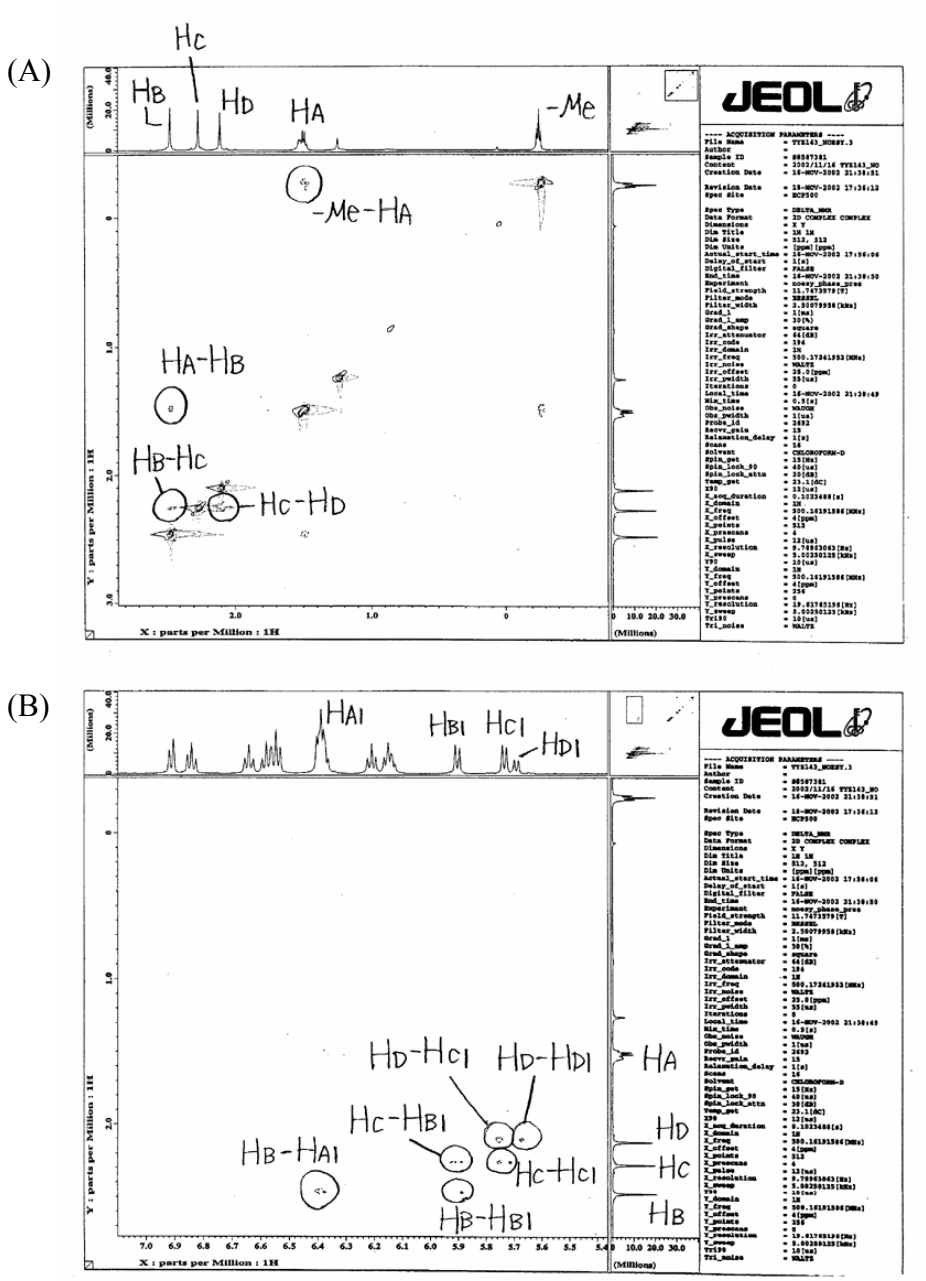

Figure 14. NOESY spectra of oligo(DBF) **2** of n = 7: alkyl-alkyl region (A) and alkyl-aromatic region (B) (500 MHz, $CDCl_3$, r.t.).

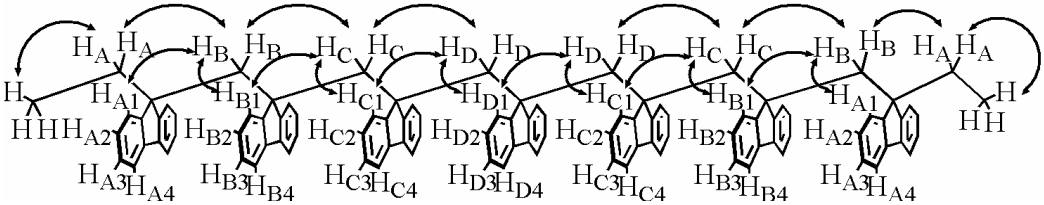

2 of n=7

(A)

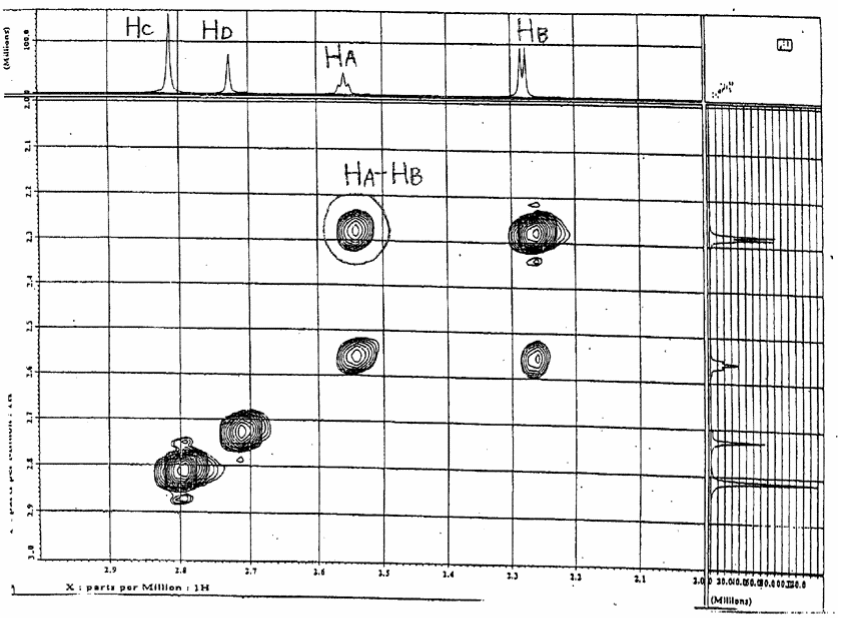

(B)

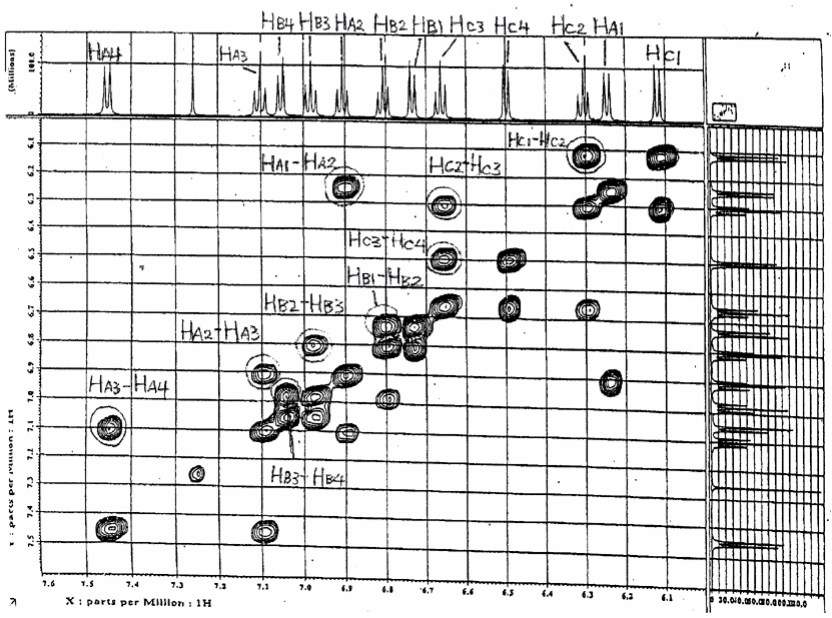

Figure S15. H-H COSY spectra of oligo(DBF) **1** of n = 6: alkyl region (A) and aromatic region (B) (600 MHz, $CDCl_3$, r.t.).

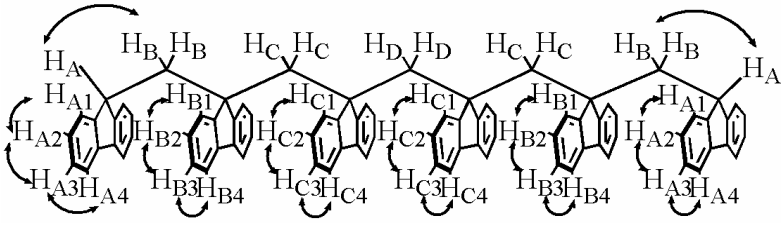

1 of n=6

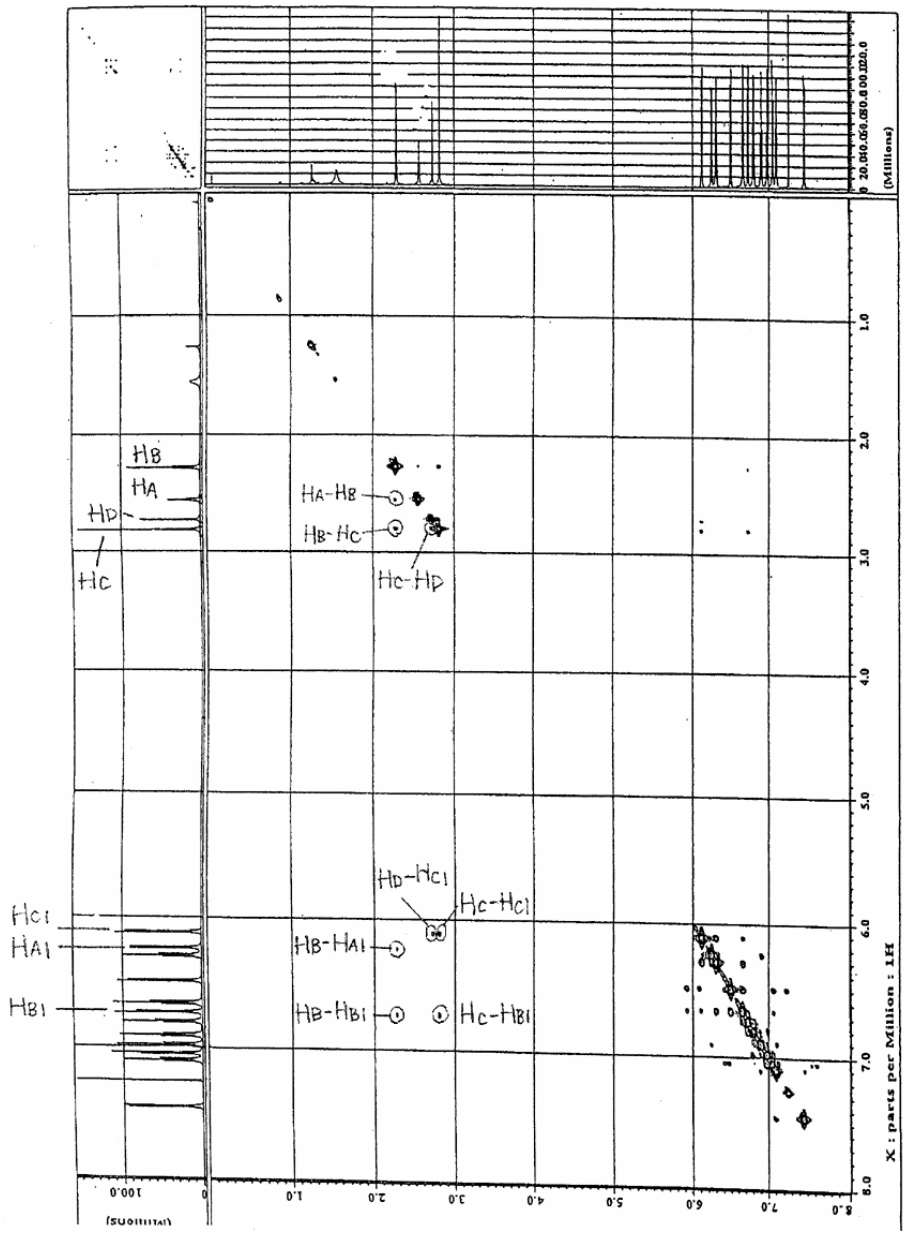

Figure S16. NOESY spectra of oligo(DBF) **1** of n = 6 (600 MHz, $CDCl_3$, r.t.).

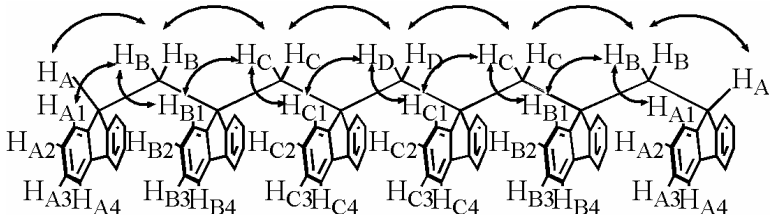

1 of n=6

(A)

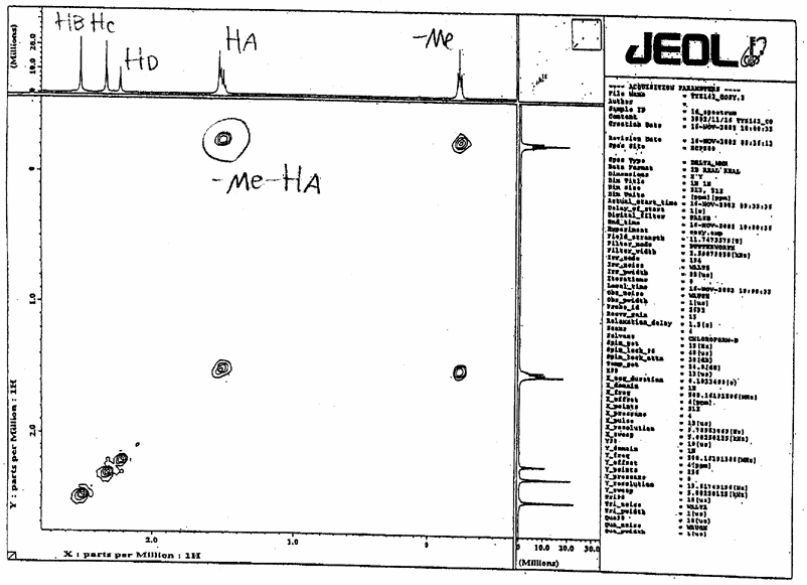

(B)

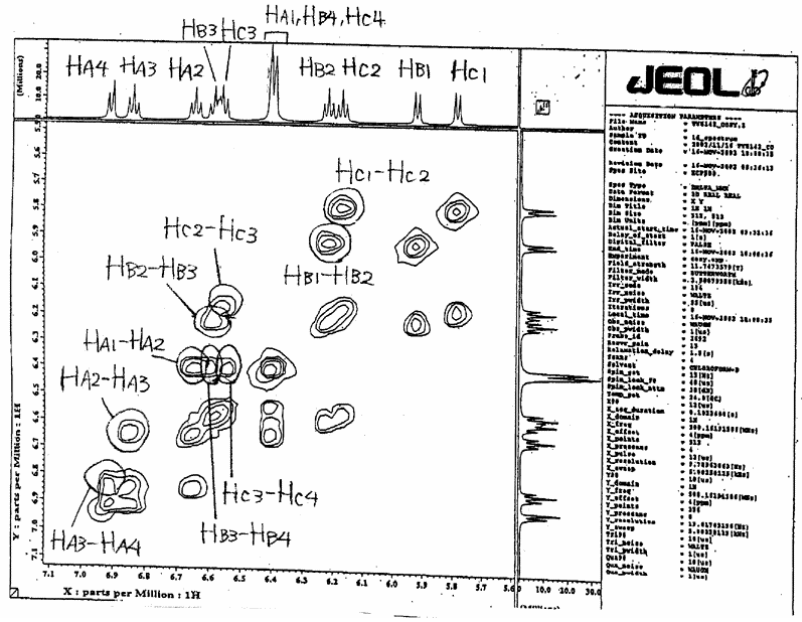

Figure S17. H-H COSY spectra of oligo(DBF) **2** of n = 6: alkyl region (A) and aromatic region (B) (500 MHz, CDCl3, r.t.).

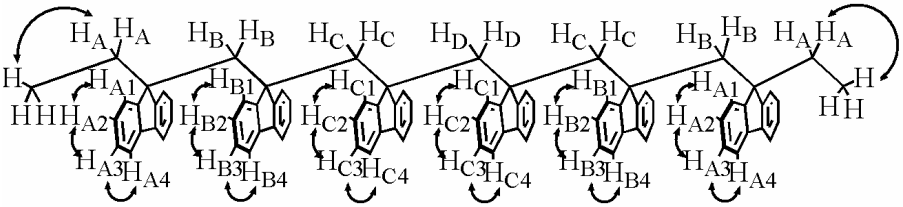

2 of n=6

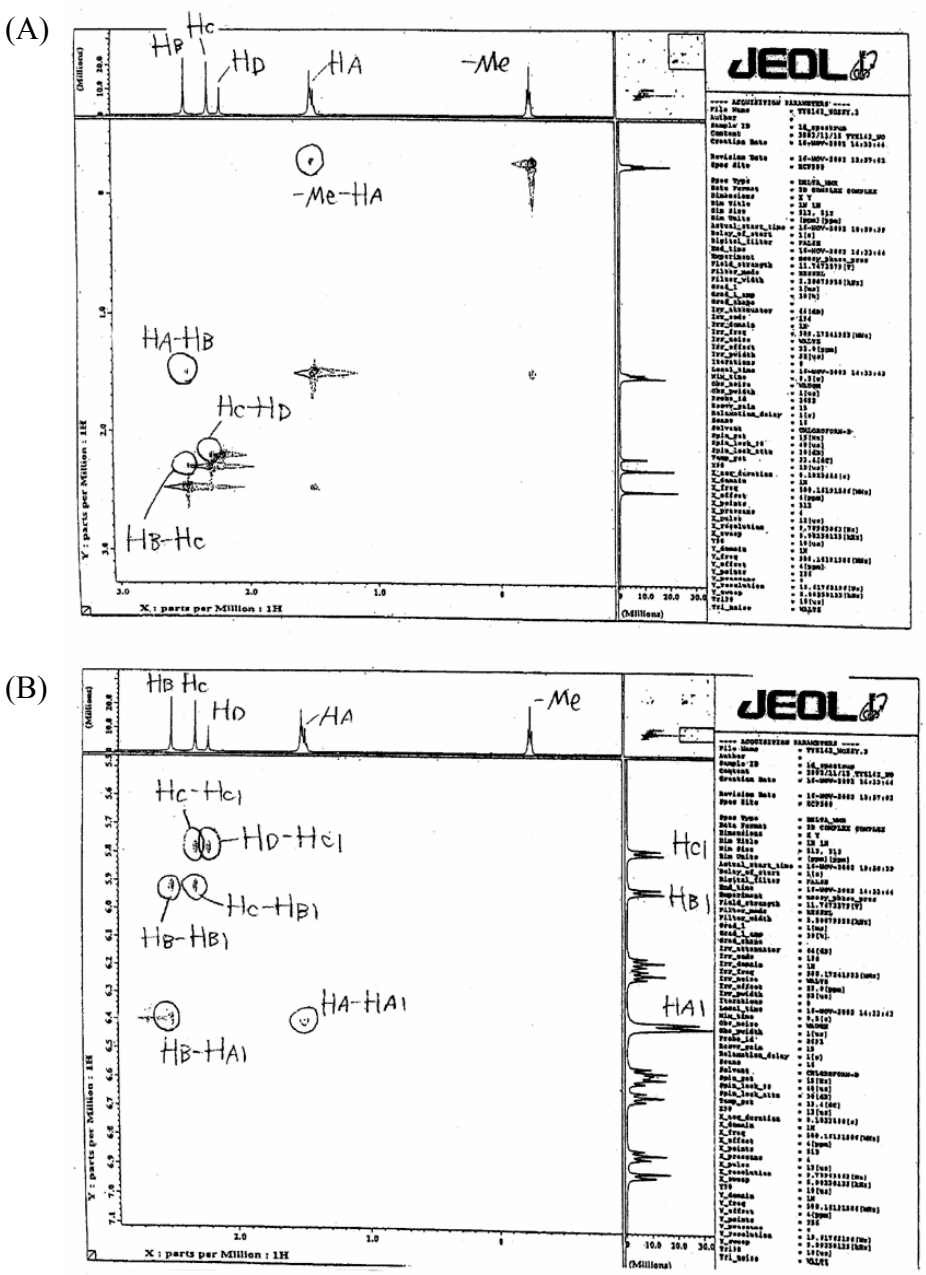

Figure S18. NOESY spectra of oligo(DBF) **2** of n = 6: alkyl-alkyl region (A) and alkyl-aromatic region (B) (500 MHz, $CDCl_3$, r.t.).

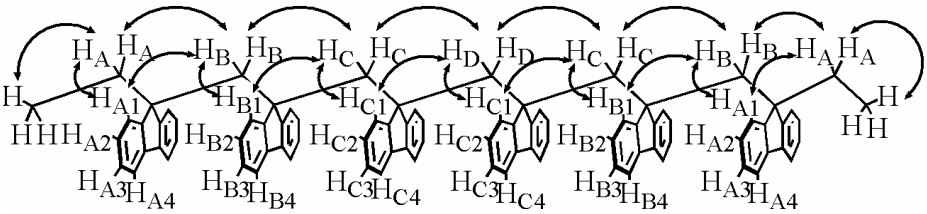

2 of n=6

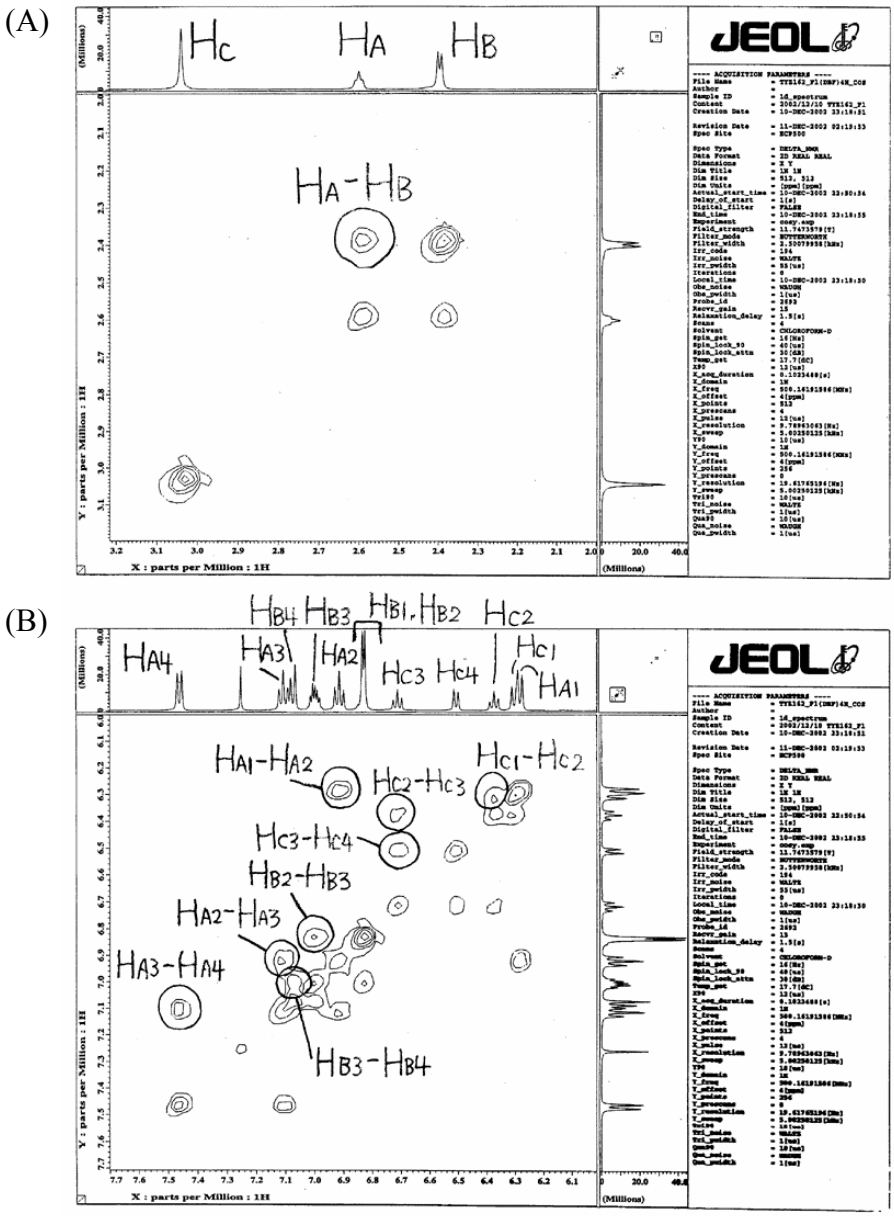

Figure S19. H-H COSY spectra of oligo(DBF) **1** of n = 5: alkyl region (A) and aromatic region (B) (500 MHz, $CDCl_3$, r.t.).

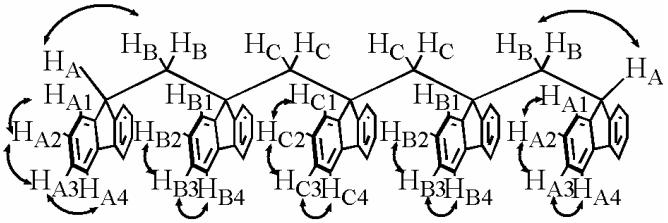

1 of n=5

(A)

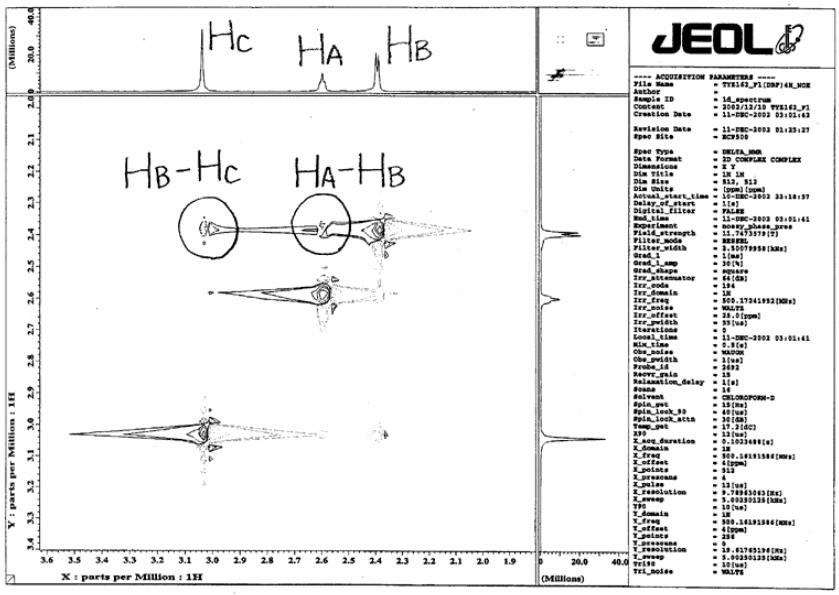

(B)

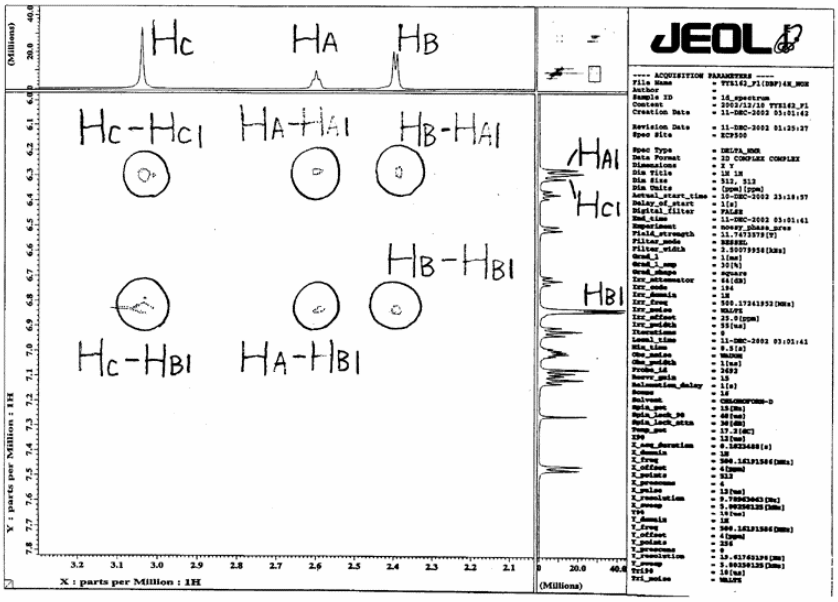

Figure S20. NOESY spectra of oligo(DBF) **1** of n = 5: alkyl-alkyl region (A) and alkyl-aromatic region (B) (500 MHz, $CDCl_3$, r.t.).

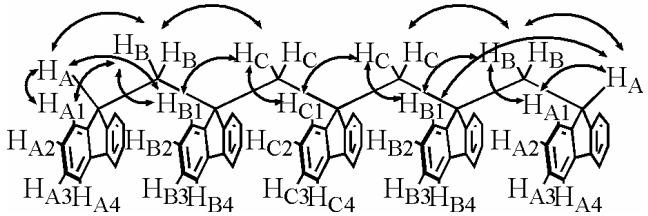

1 of n=5

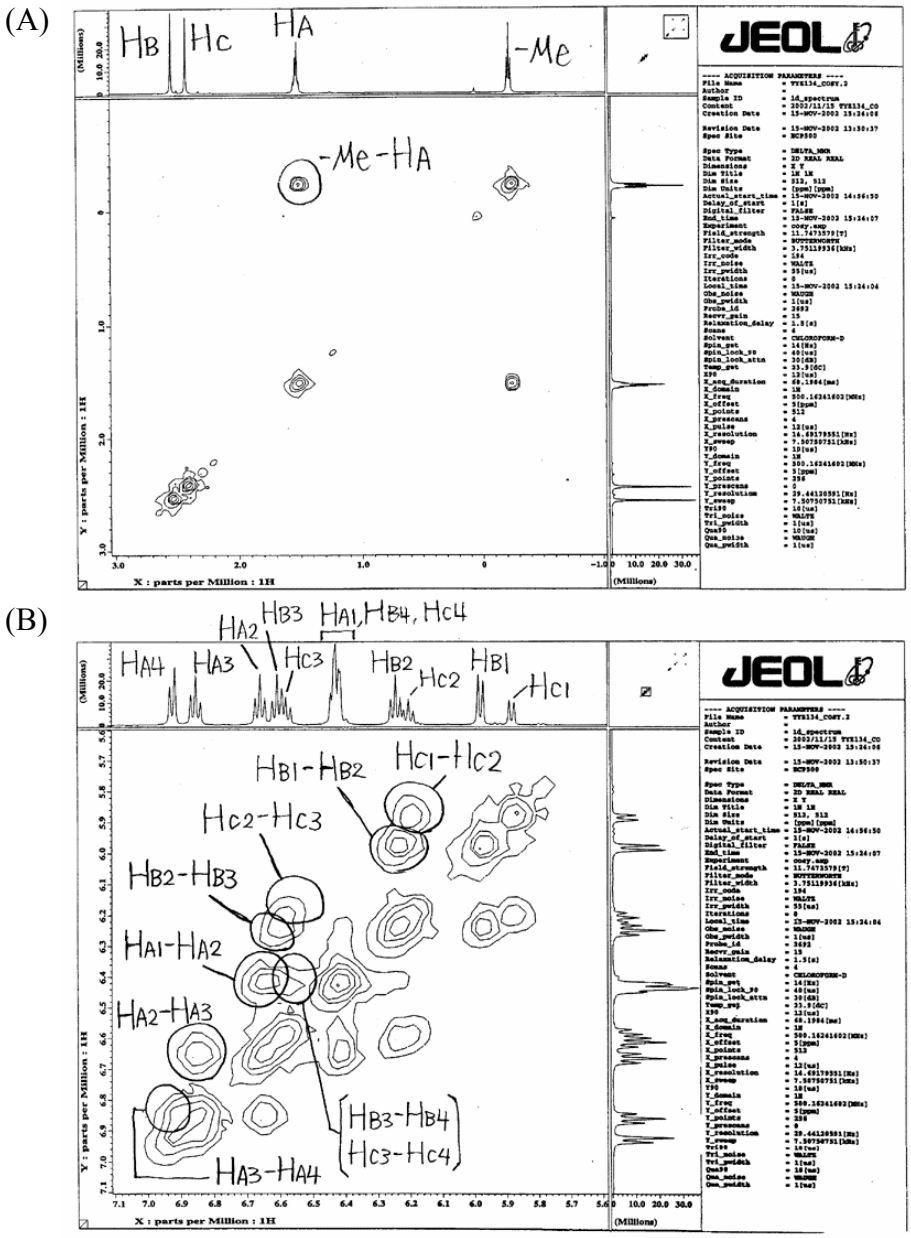

Figure S21. H-H COSY spectra of oligo(DBF) **2** of n = 5: alkyl region (A) and aromatic region (B) (500 MHz, $CDCl_3$, r.t.).

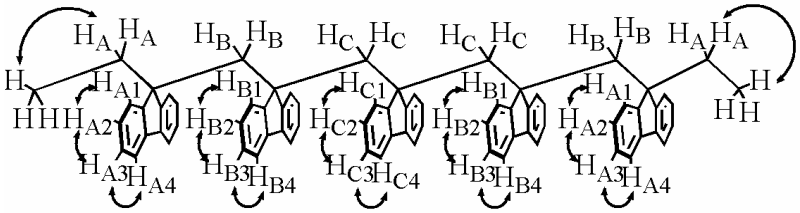

2 of n=5

(A)

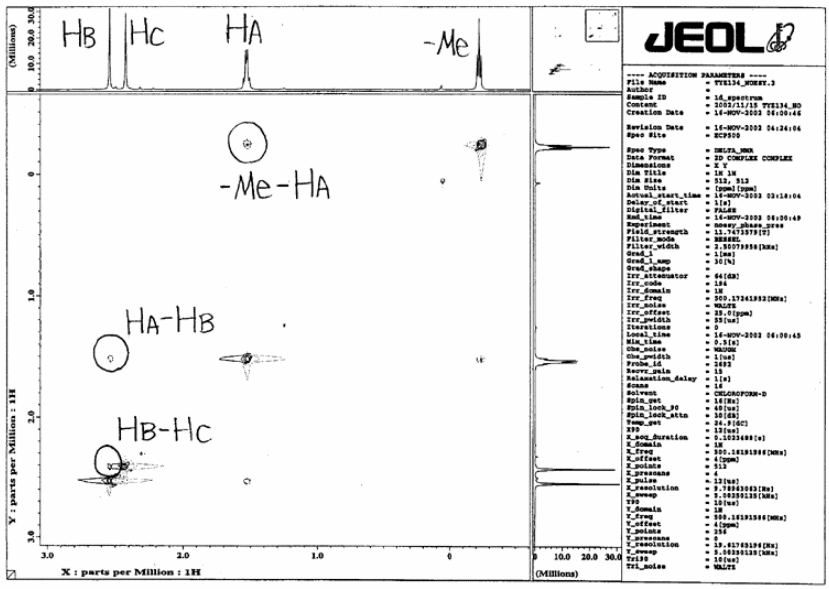

(B)

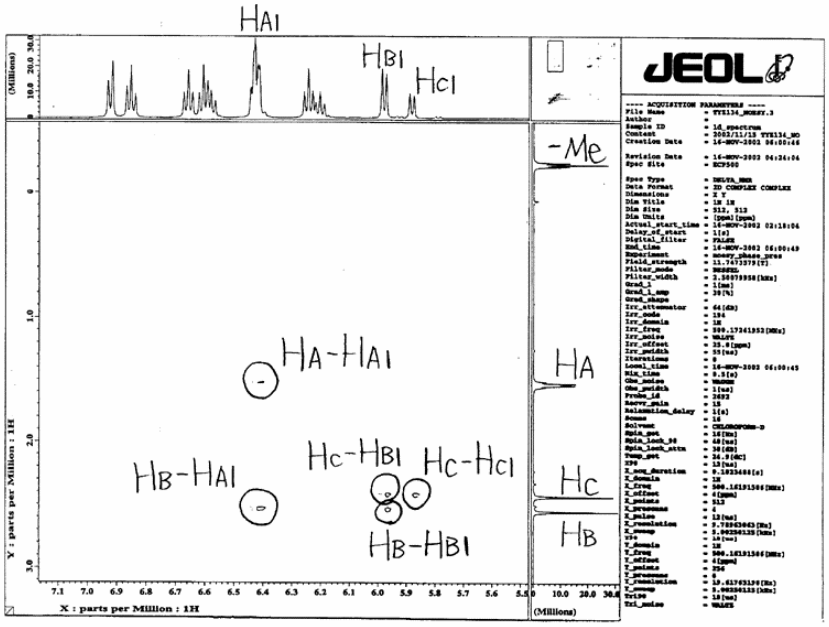

Figure S22. NOESY spectra of oligo(DBF) **2** of n = 5: alkyl-alkyl region (A) and alkyl-aromatic region (B) (500 MHz, $CDCl_3$, r.t.).

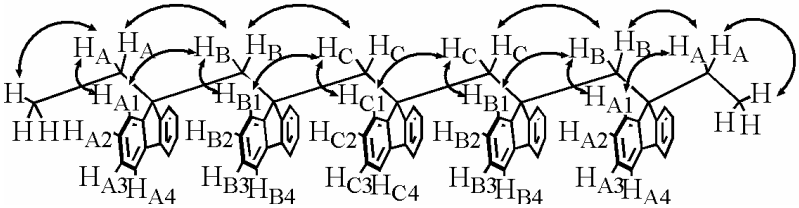

2 of n=5

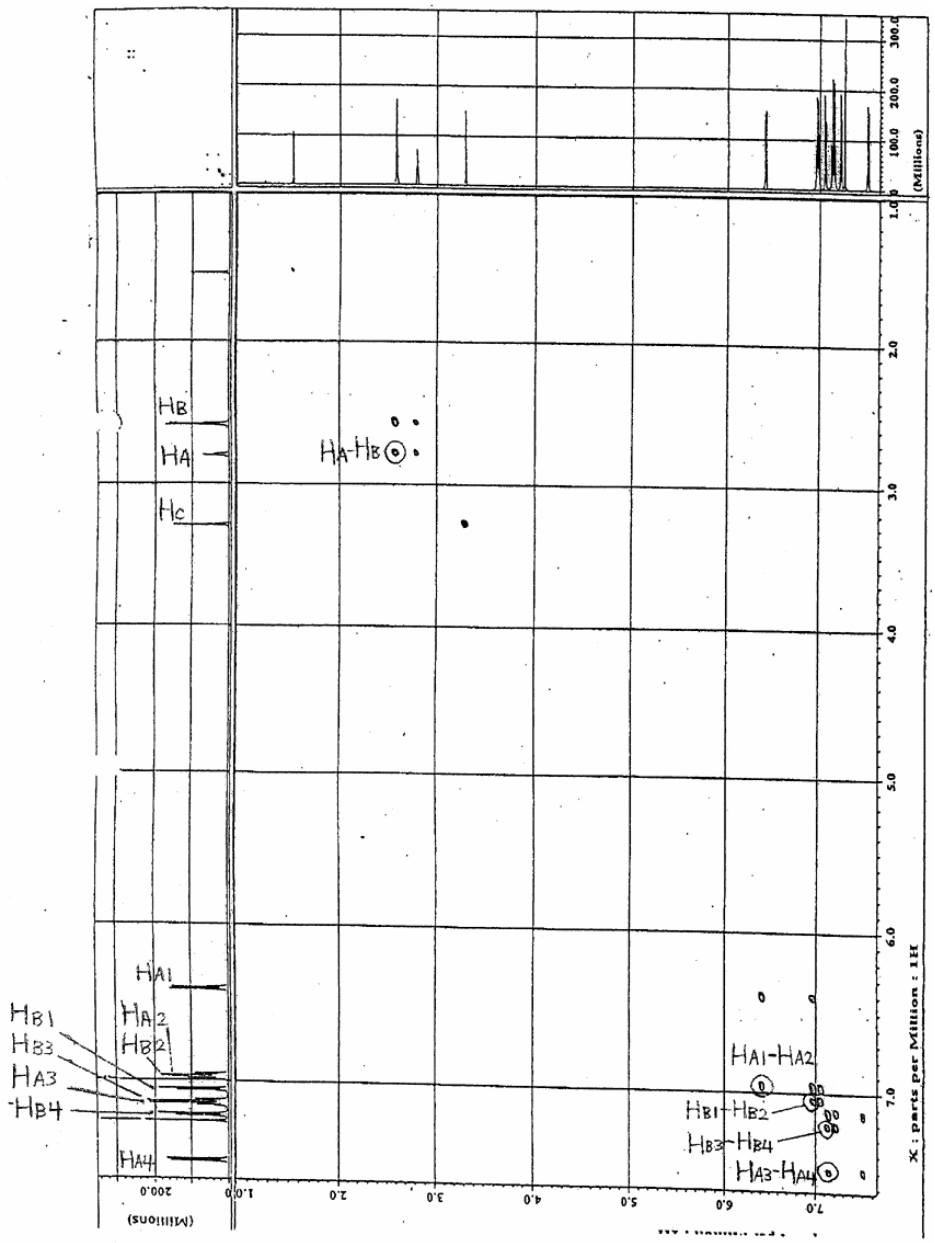

Figure S23. H-H COSY spectra of oligo(DBF) **1** of n = 4: alkyl region (A) and aromatic region (B) (600 MHz, $CDCl_3$, r.t.).

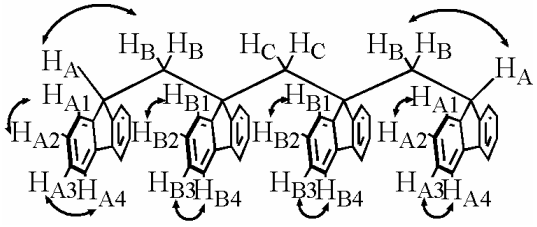

1 of n=4

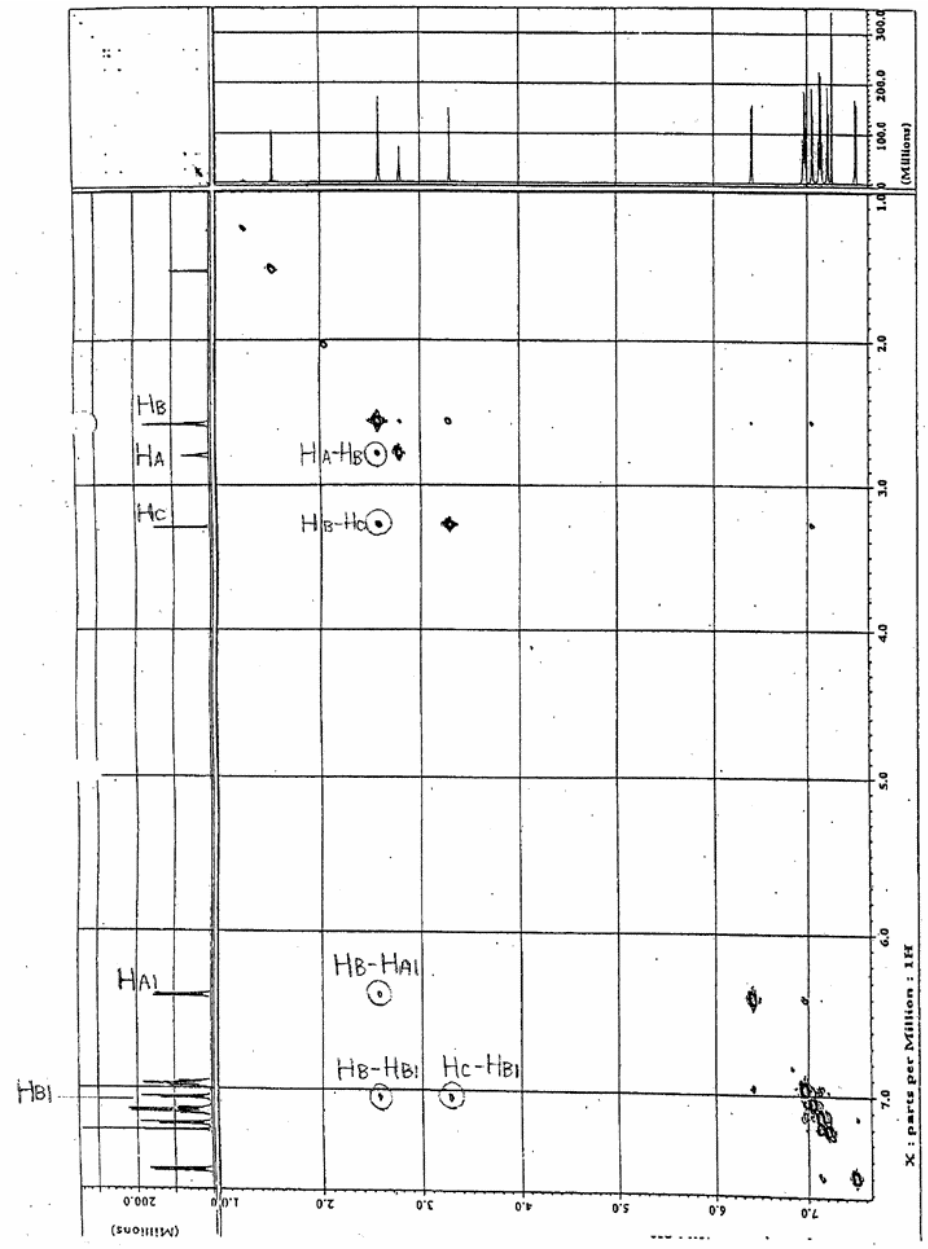

Figure S24. NOESY spectra of oligo(DBF) **1** of n = 4 (600 MHz, $CDCl_3$, r.t.).

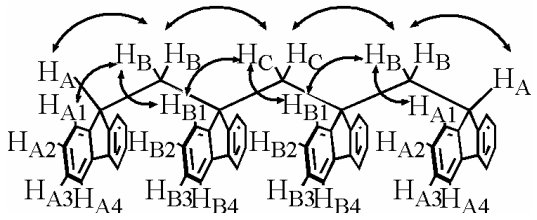

1 of n=4

(A)

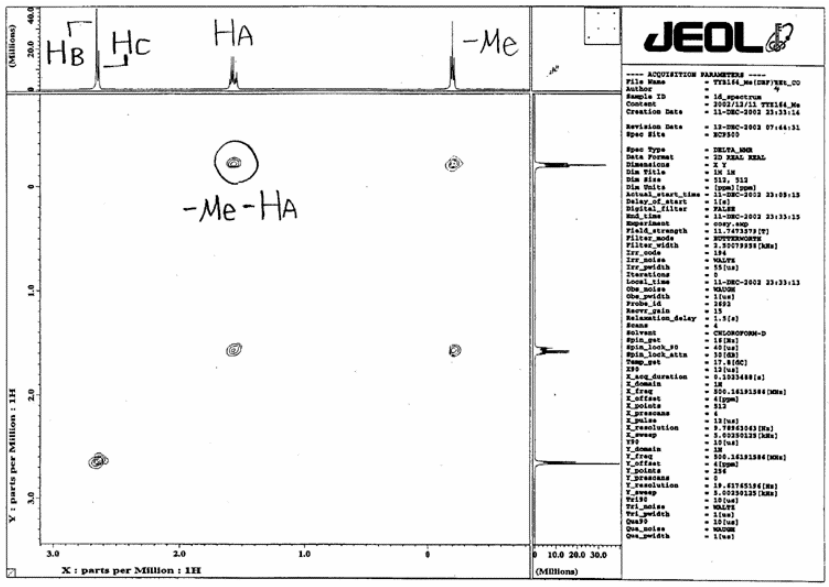

(B)

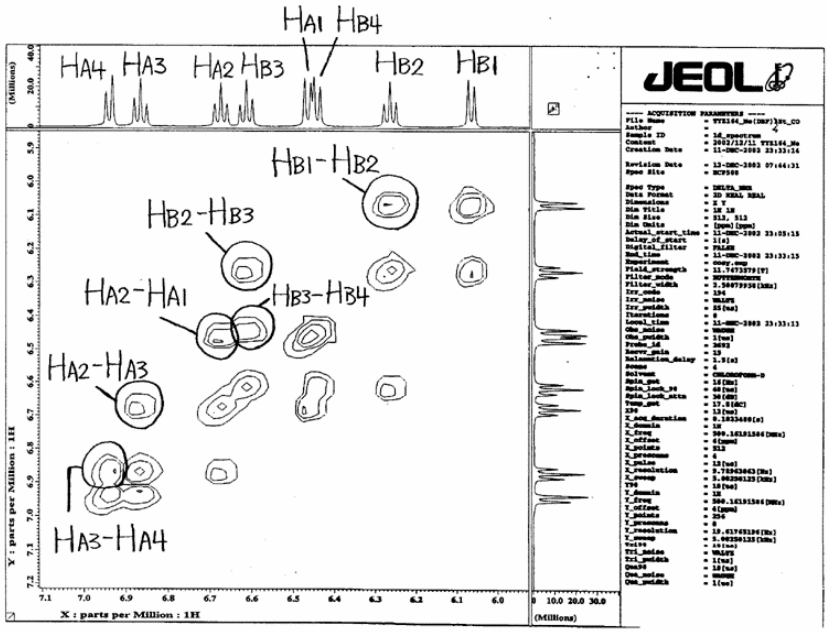

Figure S25. H-H COSY spectra of oligo(DBF) **2** of n = 4: alkyl region (A) and aromatic region (B) (500 MHz, $CDCl_3$, r.t.).

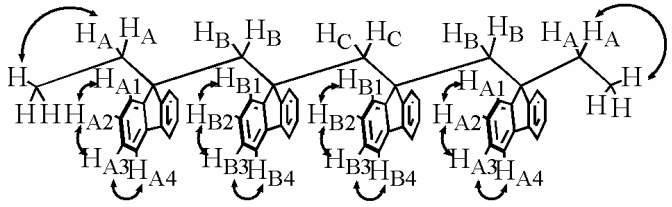

2 of n=4

(A)

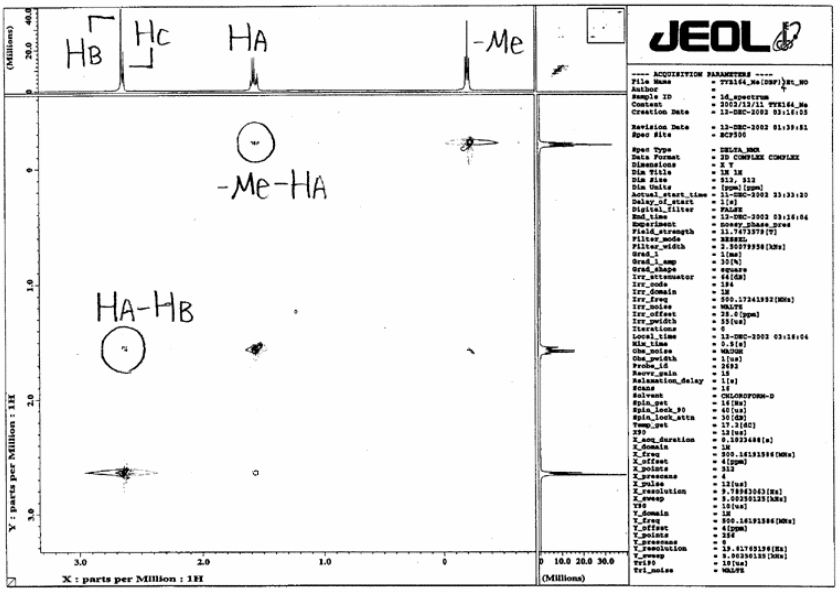

(B)

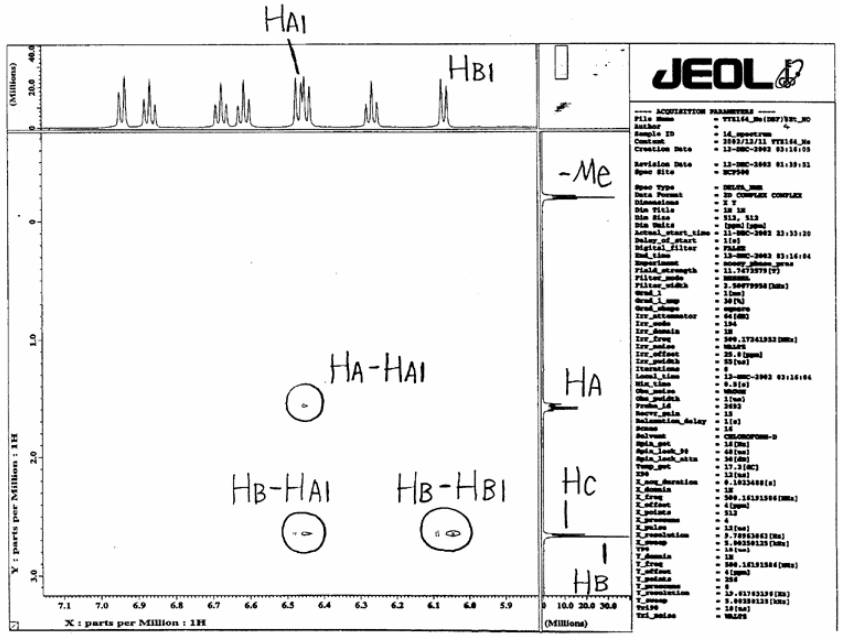

Figure S26. NOESY spectra of oligo(DBF) **2** of n = 4: alkyl-alkyl region (A) and alkyl-aromatic region (B) (500 MHz, $CDCl_3$, r.t.).

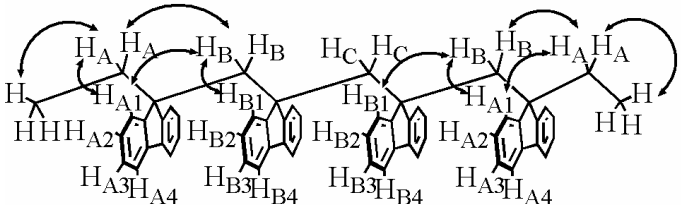

2 of n=4

(A)

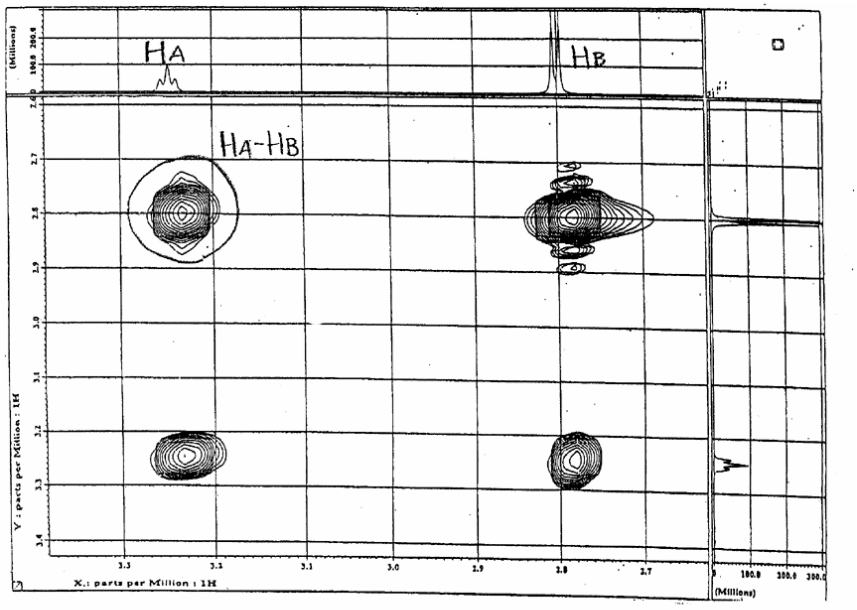

(B)

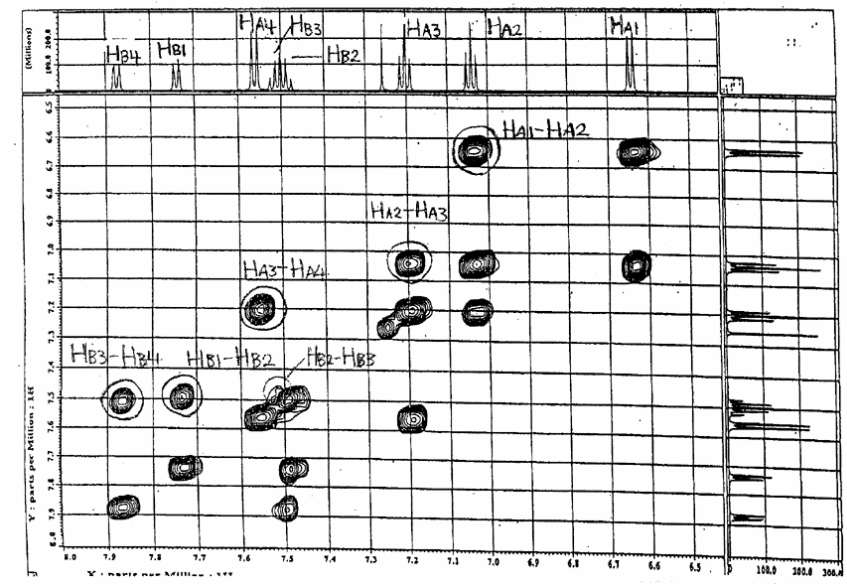

Figure S27. H-H COSY spectra of oligo(DBF) **1** of n = 3: alkyl region (A) and aromatic region (B) (600 MHz, $CDCl_3$, r.t.).

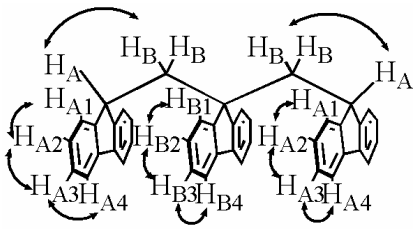

1 of n=3

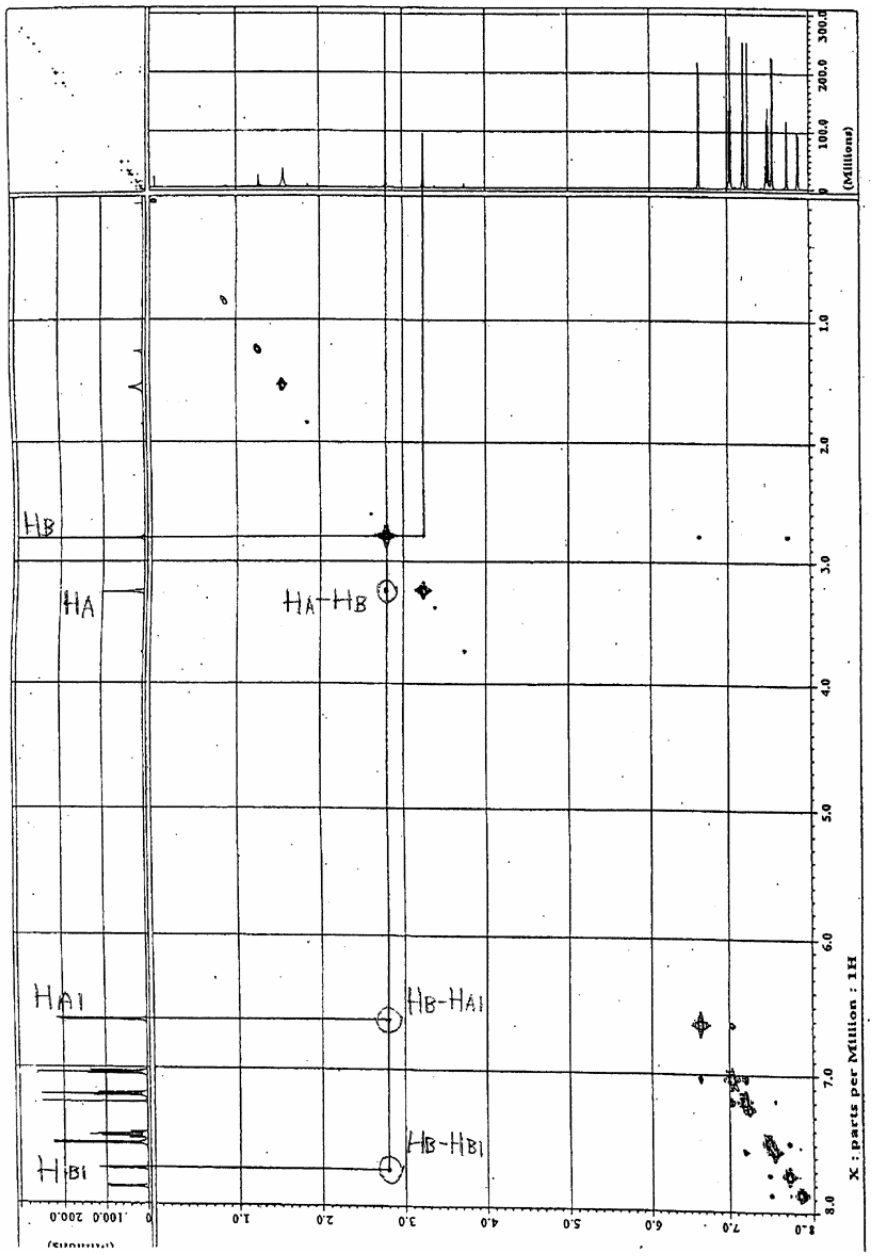

Figure S28. NOESY spectra of oligo(DBF) **1** of n = 3 (600 MHz, $CDCl_3$, r.t.).

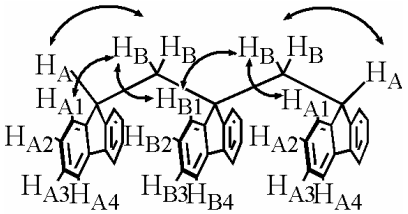

1 of n=3

(A)

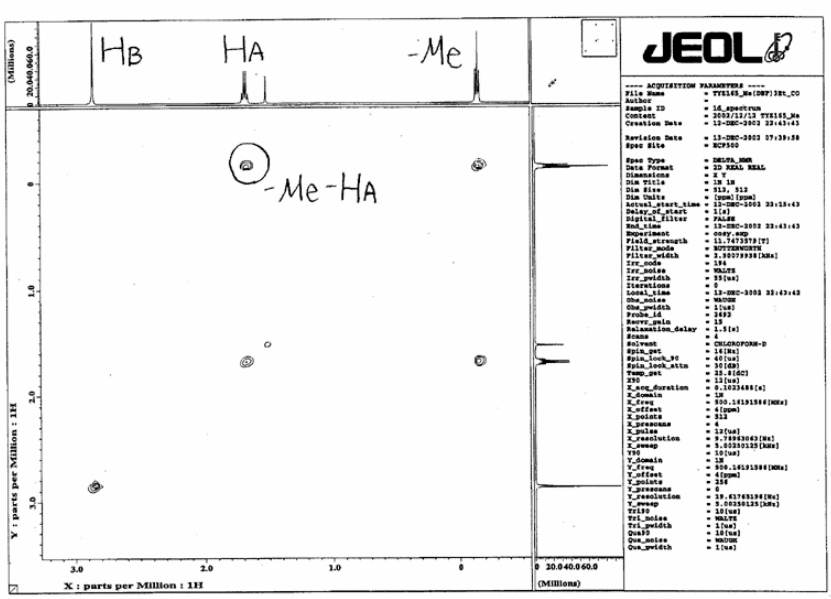

(B)

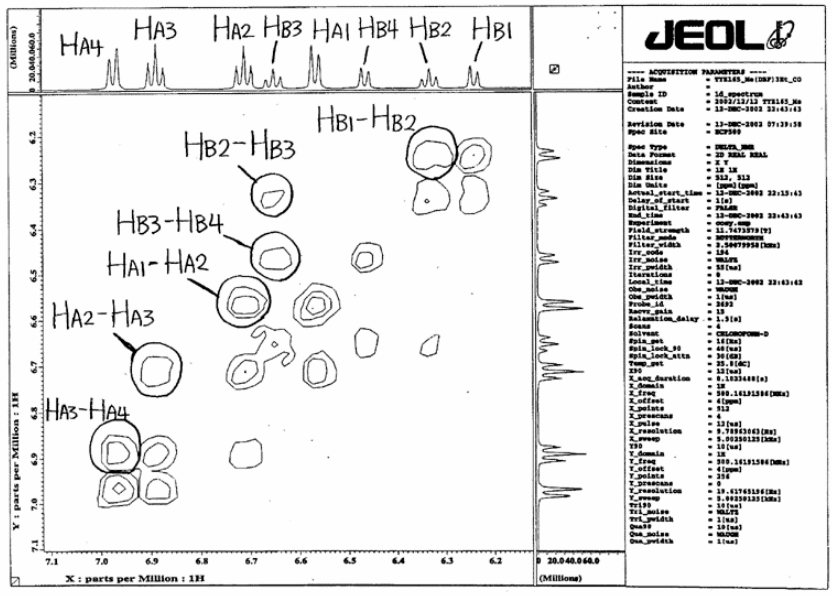

Figure S29. H-H COSY spectra of oligo(DBF) **2** of n = 3: alkyl region (A) and aromatic region (B) (500 MHz, $CDCl_3$, r.t.).

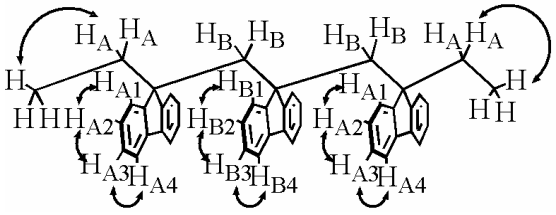

2 of n=3

(A)

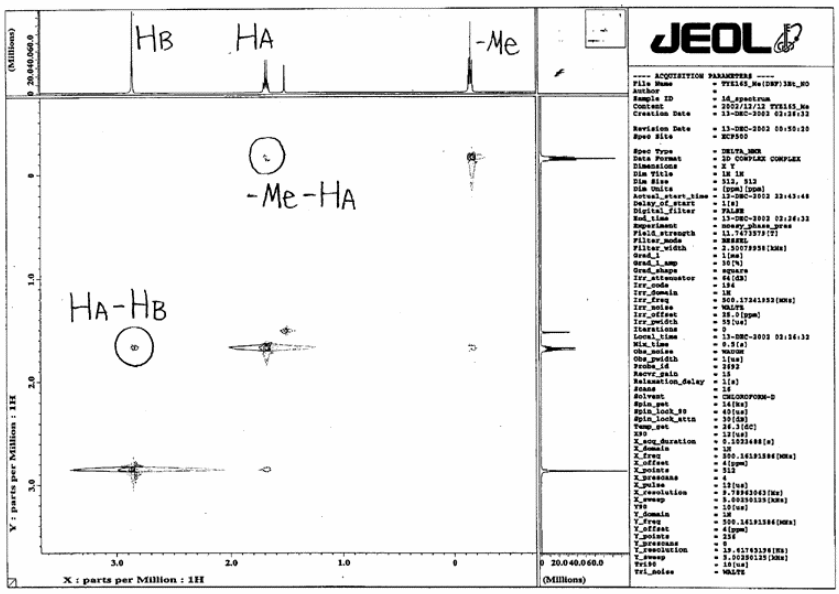

(B)

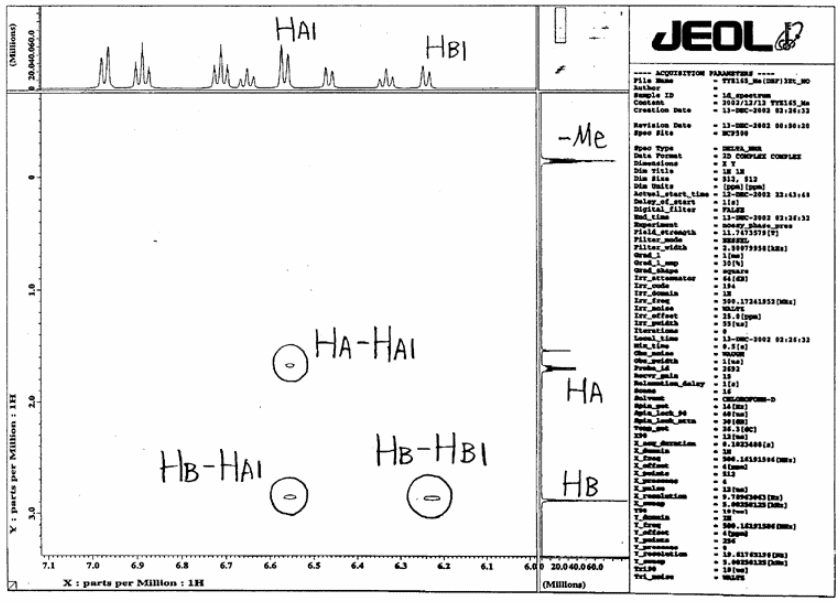

Figure S30. NOESY spectra of oligo(DBF) **2** of n = 3: alkyl-alkyl region (A) and alkyl-aromatic region (B) (500 MHz, $CDCl_3$, r.t.).

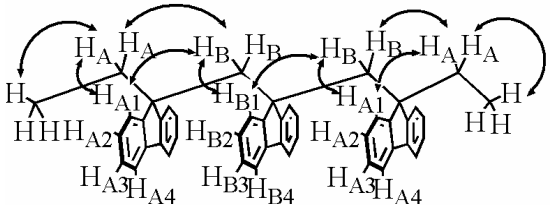

2 of n=3

(A)

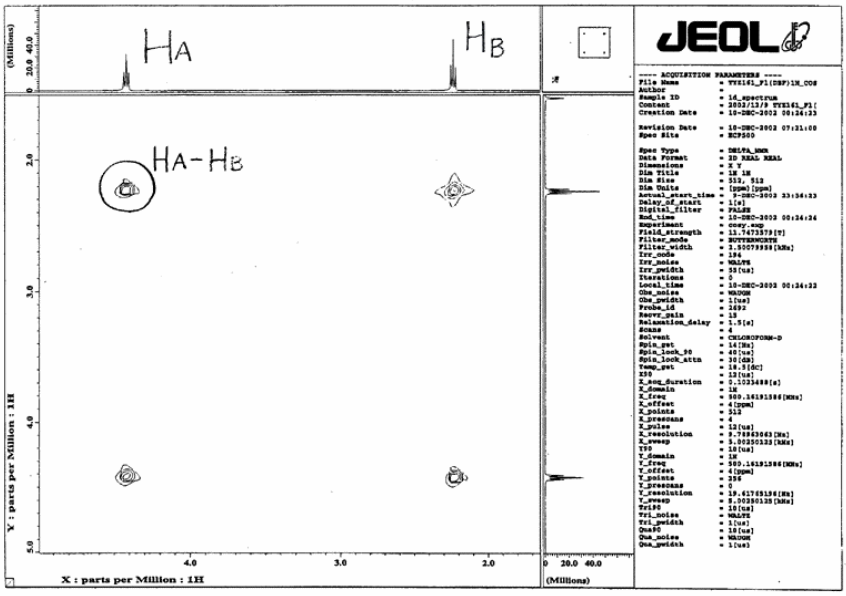

(B)

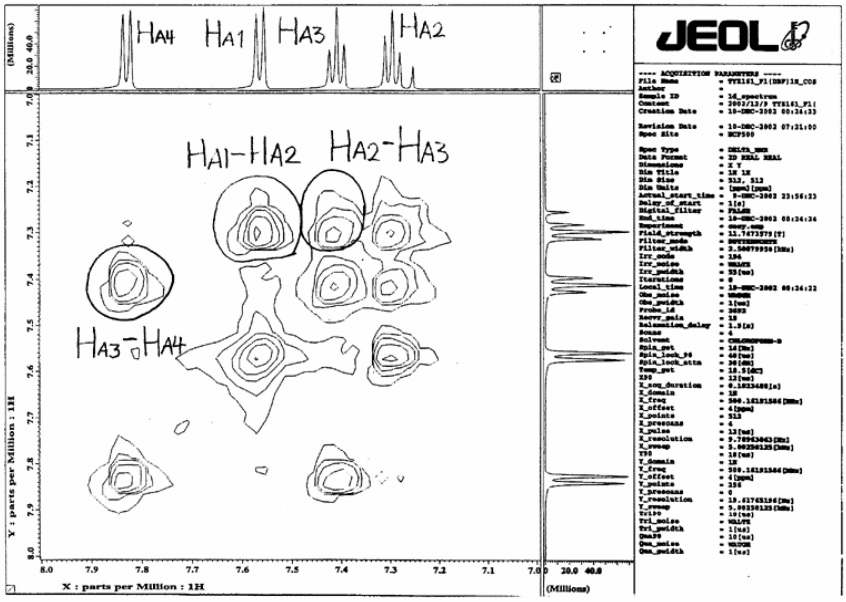

Figure S31. H-H COSY spectra of oligo(DBF) **1** of n = 2: alkyl region (A) and aromatic region (B) (500 MHz, $CDCl_3$, r.t.).

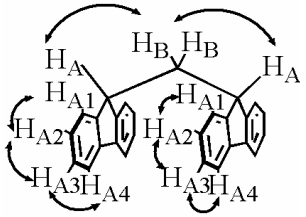

1 of n=2

(A)

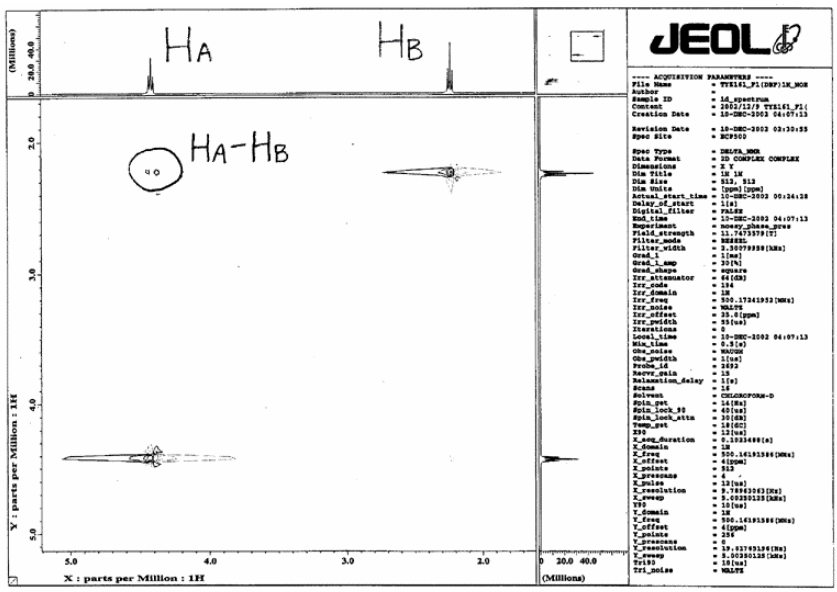

(B)

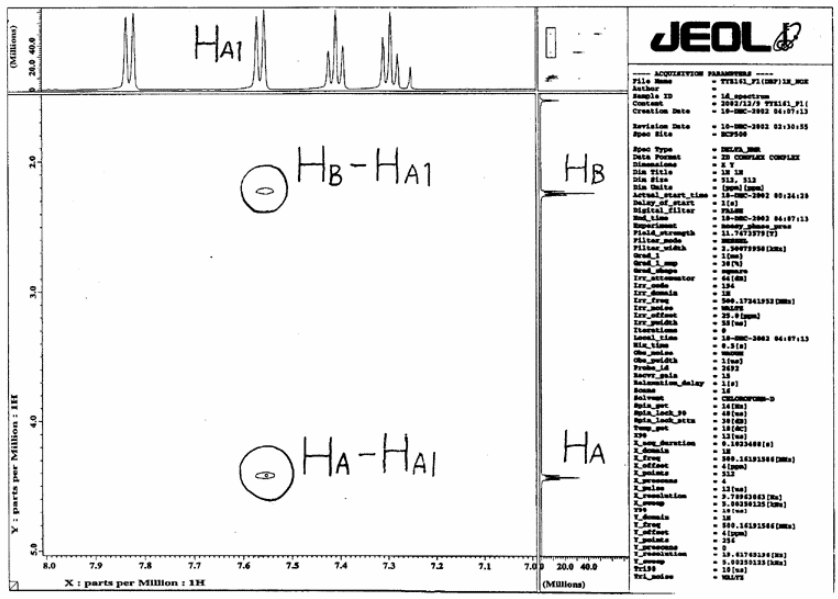

Figure S32. NOESY spectra of oligo(DBF) **1** of n = 2: alkyl-alkyl region (A) and alkyl-aromatic region (B) (500 MHz, $CDCl_3$, r.t.).

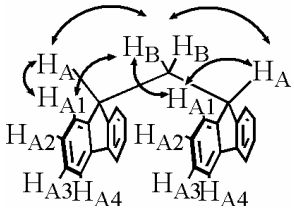

1 of n=2

(A)

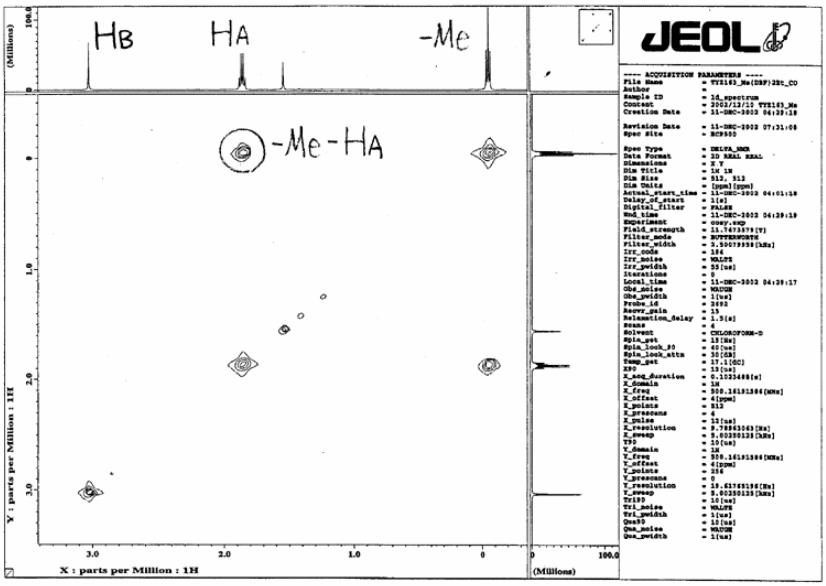

(B)

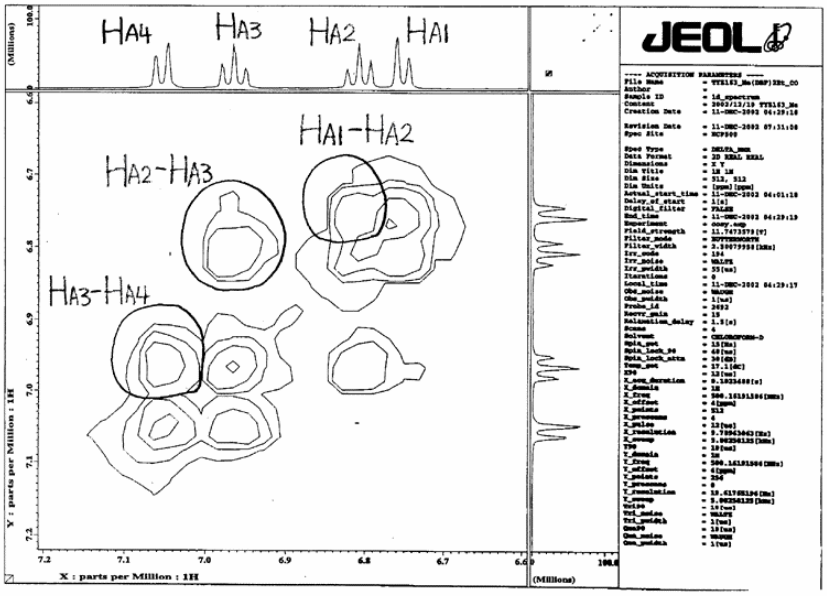

Figure S33. H-H COSY spectra of oligo(DBF) **2** of n = 2: alkyl region (A) and aromatic region (B) (500 MHz, $CDCl_3$, r.t.).

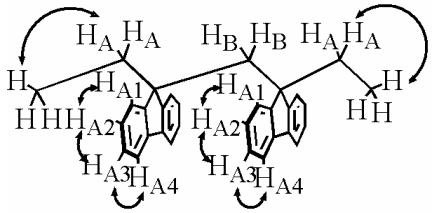

2 of n=2

(A)

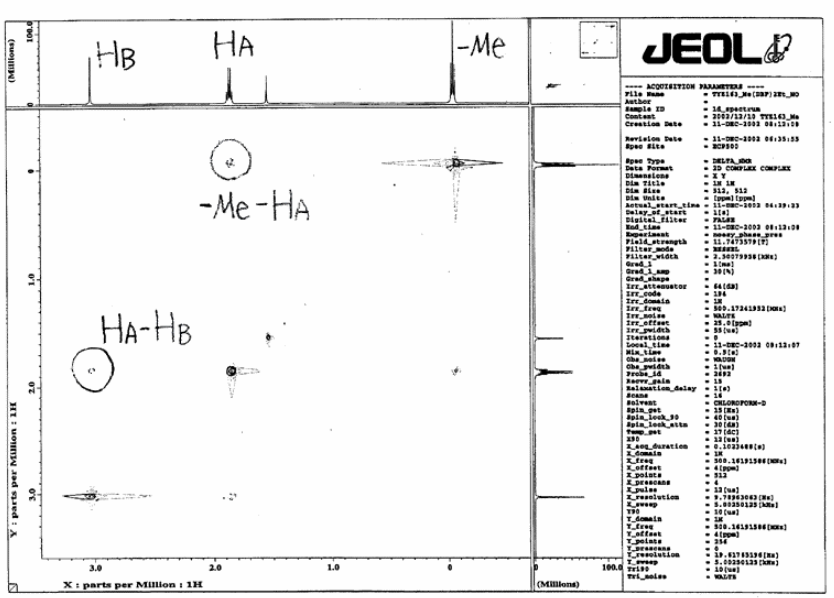

(B)

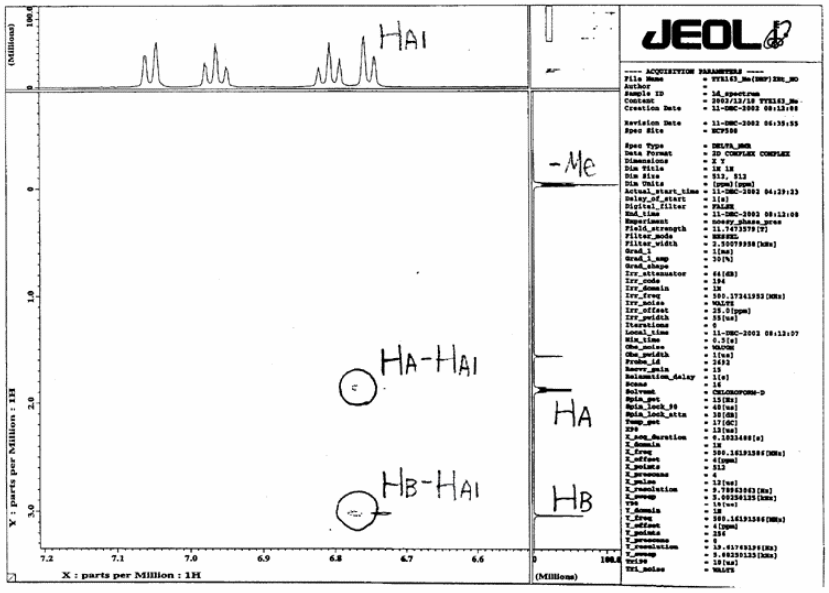

Figure S34. NOESY spectra of oligo(DBF) **2** of n = 2: alkyl-alkyl region (A) and alkyl-aromatic region (B) (500 MHz, $CDCl_3$, r.t.).

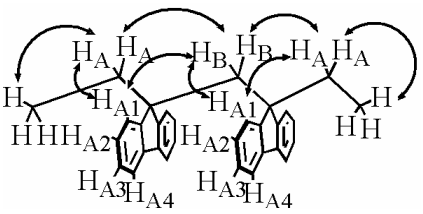

2 of n=2